

Aus dem Institut für Systemische Neurowissenschaften  
der Heinrich-Heine-Universität Düsseldorf  
Direktor: Univ.-Prof. Dr. med. Simon B. Eickhoff

Organization of the human cerebral neurotransmission  
landscape

Dissertation

zur Erlangung des Grades eines Doktors der Medizin  
der Medizinischen Fakultät der Heinrich-Heine-Universität  
Düsseldorf

vorgelegt von

Benjamin Hänisch

2024

Als Inauguraldissertation gedruckt mit Genehmigung der Medizinischen Fakultät der  
Heinrich-Heine-Universität Düsseldorf

gez.:

Dekan: Prof. Dr. med. Nikolaj Klöcker

Erstgutachter: Prof. Dr. rer. med. Juergen Dukart

Zweitgutachter: PD Dr. med. Nico Melzer

Drittgutachter: Prof. Dr. med. Florian Schlagenhaut, MA



## **Auflistung der Publikationen**

Teile dieser Arbeit wurden veröffentlicht:

Hänisch B., Hansen J.Y., Bernhardt B.C., Eickhoff S.B., Dukart J., Misic B., Valk S.L. (2023): Cerebral chemoarchitecture shares organizational traits with brain structure and function. eLife, <https://doi.org/10.7554/eLife.83843> (1)

## **Zusammenfassung**

Systematische neuroanatomische Untersuchungen sind ein wichtiger Pfeiler der Neurowissenschaften. Diese Arbeit untersucht die Chemoarchitektur - die Verteilung von Neurotransmitter-Rezeptoren und -Transportern im menschlichen Gehirn. Der Grad interregionaler chemoarchitektonischer Ähnlichkeit im Kortex und subkortikalen Kernen, wird quantifiziert und als neue Metrik „Rezeptom“ eingeführt. Hierzu wird ein frei zugänglicher Datensatz von Dichtekarten aus der Positronen-Emissions-Tomographie verwendet, der Daten von über 1200 Probanden enthält und 19 verschiedene Rezeptoren und Transporter abdeckt. Aus der hochdimensionalen Rezeptom-Matrix werden durch nichtlinearer Dimensionsreduktionsalgorithmen sogenannte Gradienten extrahiert - räumliche Verteilungsmuster, die die Hauptachsen chemoarchitektonischer Varianz beschreiben. Drei Gradienten werden verwendet, um das Verhältnis verschiedener Hirnareale zueinander auf der Grundlage ihrer chemoarchitektonischen Ähnlichkeitsprofile zu untersuchen. Rezeptor- und Transporter-Ko-Verteilungsmuster, die für chemoarchitektonische Differenzierung ausschlaggebend sind, werden identifiziert. Funktionelle Dekodierung zeigt, dass chemoarchitektonische Gradienten Kortizes mit unimodaler und transmodaler Funktionalität differenzieren. Weiterhin zeigen sie signifikante Korrelationen zu morphologischen Veränderungen des Kortex, die mit psychiatrischen Störungen assoziiert sind. Darüber hinaus überlappen die Verteilungsmuster chemoarchitektonischer Gradienten signifikant mit denen aus funktioneller und struktureller Konnektivität sowie aus zytoarchitektonischen Differenzierungsdaten gewonnener Gradienten. Auf der Parcel-Ebene werden cytoarchitektonische Eigenschaften den vorher genannten Maße entlang eines idiotypischen-nach-paralimbischen Gradienten zytoarchitektonischer Klassen unähnlicher. Heteromodale Kortizes weisen eine größere Rezeptom-Heterogenität als paralimbische Kortizes auf. Schließlich können die Funktionsgemeinschaften subkortikaler Kerne anhand ihrer chemoarchitektonischen Merkmale unterschieden werden, wodurch im Kortex bekannte, rezeptorbasierte Struktur-Funktions-Beziehungen auch im subkortikalen Bereich nachgewiesen werden. Zusammenfassend nutzt diese Arbeit frei verfügbare *in-vivo*-Daten, um die neuartige neuroanatomische Perspektive des Rezeptoms zu entwickeln und zu untersuchen.

## Summary

The systematic study of anatomical features of the brain is a long-standing and important pillar of neuroscience. This study investigates chemoarchitecture, the distribution of neurotransmitter receptors and transporters in the human brain, in a systematic fashion. It introduces a novel neuroanatomical perspective through quantifying the degree of inter-regional chemoarchitectural similarity in the cortex and subcortical nuclei, deriving a metric it terms the “receptome”. To investigate cerebral chemoarchitecture, a large-scale, open-access dataset of Positron Emission Tomography-derived density maps is used, featuring data from over 1200 subjects and covers 19 different receptors and transporters. From the high-dimensional receptome matrix, non-linear manifold learning techniques extract principal gradients, spatial patterns that cover the main axes of chemoarchitectural variation. Three of these gradients are subsequently employed to gain a deeper understanding of the relationship between different cortices based on their chemoarchitectural similarity profiles. Receptor and transporter co-distribution patterns that drive chemoarchitectural differentiation are delineated in the cortex and in subcortical nuclei. Functional decoding reveals that chemoarchitectural similarity gradients differentiate between cortices of unimodal and transmodal functionality. The gradients also show significant correlations to cortical morphological alterations found in psychiatric disorders and share spatial characteristics that significantly overlap with gradients derived from functional connectivity, structural connectivity, and cytoarchitectural differentiation data. On the parcel level, chemoarchitectural similarity dissociates from the aforementioned measures along an idiotypic-to-paralimbic gradient of cytoarchitectural classes. Heteromodal cortices show higher receptomic heterogeneity than paralimbic cortices. Finally, functional communities of subcortical nuclei are separated by their chemoarchitectural characteristics, expanding receptor-based structure-function relationships known in the cortex to the subcortical domain. Summarized, this study uses *in-vivo* open-access data to generate and investigate the receptome as a novel neuroanatomical mode.

## List of abbreviations

5-HT2a	5-Hydroxytryptamine receptor 2a
5-HT2b	5-Hydroxytryptamine receptor 2b
5-HTT	5-Hydroxytryptamine transporter
5-HTTLPR	Serotonin-transporter-linked promoter region
AMPA	alpha-amino-3-hydroxy-5-methyl-4-isoxazolepropionic acid
BOLD	Blood-Oxygen-Level-Dependent
D1	Dopamine receptor D1
D2	Dopamine receptor D2
DAT	Dopamine transporter
dMRI	Diffusion-weighted Magnetic Resonance Imaging
ENIGMA	Enhancing NeuroImaging Genetics through Meta-Analysis
FC	Resting-state Functional Connectivity
fMRI	Functional Magnetic Resonance Imaging
GABA	gamma-Aminobutyric acid
GABAa	gamma-Aminobutyric acid receptor a
LSD	Lysergic acid diethylamide
MPC	Microstructural Profile Covariance
MRI	Magnetic Resonance Imaging
NAT	Noradrenaline transporter
NMDA	N-methyl-D-aspartate receptor
NTRM	Neurotransmitter transporter or receptor molecule
PCA	Principal Component Analysis
PET	Positron Emission Tomography
RC	Receptome
SC	Structural Connectivity
SSRI	Selective Serotonin Reuptake Inhibitor

## Table of contents

<b>1 Introduction</b> .....	<b>1</b>
1.1 Studies of brain structure and function .....	1
1.1.1 Cytoarchitectural mapping .....	1
1.1.2 Imaging-based anatomical modes .....	3
1.1.3 Other brain mapping efforts .....	4
1.2 Neurotransmitter systems in the human brain.....	6
1.2.1 Neurotransmitter mapping.....	6
1.2.2 Functional relevance of neurotransmission and neurotransmitter mapping.....	7
1.2.3 Relevance of neurotransmitter systems in clinical medicine .....	8
1.3 Aims of this work.....	8
<b>2 Publication:</b> Hänisch B., Hansen J.Y., Bernhardt B.C., Eickhoff S.B., Dukart J., Misić B., Valk S.L.: Cerebral chemoarchitecture shares organizational traits with brain structure and function; eLife (2023) .....	<b>10</b>
<b>3 Discussion</b> .....	<b>11</b>
3.1 Principal gradients in brain organization .....	11
3.2 The organization of cortical chemoarchitecture.....	12
3.2.1 Cortical anatomy as defined by chemoarchitectural similarity gradients .....	12
3.2.2 Functional decoding of chemoarchitectural similarity axes.....	12
3.2.3 Disease-related aspects of chemoarchitecture .....	13
3.3 Chemoarchitecture as an anatomical layer.....	15
3.4 Limitations .....	16
3.5 Conclusions and outlook .....	18
<b>4 References</b> .....	<b>19</b>

## **1. Introduction**

### **1.1 Studies of brain structure and function**

The study of human brain anatomy has been paramount in understanding how the brain's function is supported by its structure (2). Neuroanatomical brain mapping efforts have a rich history, having progressed from early histology-based systematic cartographies of the cortex to continuously refining our understanding of cerebral anatomy by using modern technology. This study introduces a novel approach to neuroanatomical mapping based on chemoarchitectural properties. Chemoarchitecture refers to the distribution of neurotransmitter transporter or receptor molecules (NTRM) in the brain. As this study has to be read against the background of the brain mapping subdiscipline, a short overview of main anatomical modes and their implications for structure-function relationships will be provided.

#### **1.1.1 Cytoarchitectural mapping**

The first systematic studies of regional cortical variability focused on histological characteristics. The most prominent early studies were conducted by Cécile and Oskar Vogt, who studied myeloarchitecture, the histological variability based on the myelin fiber content, and their collaborator Korbinian Brodmann, who worked on cartography of the cortex based on changes in the cellular and laminar composition. Brodmann published an influential cortical parcellation based on regional variations in cytoarchitectural characteristics in 1909 (3), while the Vogts published a myeloarchitecture-based cortical map 1919 (4). The cytoarchitectonic approach has enjoyed more prominence, and Brodmann's originally defined 43 cortical areas are still in use in clinical terminology today. His systematic dissection of histological profiles was improved and expanded on in later work (5–7). Core findings from these early studies remain relevant – horizontally, the cerebral cortex consists of cytoarchitectural layers, and vertically, variations in histological composition can be used to detect cytoarchitectural local communities.

Methodological advances have allowed for new levels of detail and rigorousness in brain mapping based on histological characteristics. Technological advancements enabled controlling for inter-individual differences (8) and a standardized rating of what constitutes

cytoarchitectural borders (9), ameliorating the inter-rater variability inherent to pure visual inspection and enabling a statistically testable and quantifiable assessment of variation in cellular composition. Advancements in histochemical staining have also been employed in cytoarchitectural brain mapping. Cell-type specific staining can be achieved through immuno-histochemistry, where targeted labeling of structures of interest is possible through fluorescence-labeled antibodies. For example, immuno-histochemistry has enabled a detailed mapping of the cerebral distribution of cholinergic neurons, touching on a neurochemical aspect of cytoarchitecture (10). Further differentiation can be achieved by investigating the transcriptional landscape of cortical areas. One of the most advanced efforts to perform whole-brain transcriptomic mapping in the cortical surface is the Allen Human Brain Atlas (11). It offers a first comprehensive analysis of the human brain transcriptome, albeit from relatively thick brain slices (0.5-1cm).

The most modern approach of generating a cytoarchitectural whole-brain map was undertaken by the BigBrain initiative (12). In this large-scale international project, a post-mortem adult human brain was imaged with MRI *in cranio*, and subsequently formalin fixed, sliced in sections on 20 $\mu$ m, Nissl stained and then histologically imaged. This combination of high-resolution microscopic and MRI imaging is a first step towards leveraging modern computing resources to reach unprecedented levels of detail on a large scale and enable the 3D reconstruction of 2D histological slices.

Furthermore, cyto- and myeloarchitectural proxy measures derived from MR images can complement histological studies by sacrificing resolution for a higher throughput and the ability to perform *in-vivo* measurements of cytoarchitecture. Cortical myelin content can be inferred from the ratio between T1- and T2-weighted MR images (13,14), or from quantitative T1 imaging (15). Measurements of cortical microstructure extracted from MR imaging and histological studies largely overlap, as demonstrated using BigBrain data (16). MRI-based cytoarchitectural measurement can therefore complement modern histological approaches, as these two methods show opposite distributions of strengths and weaknesses.

### 1.1.2 Imaging-based anatomical modes

#### *Functional Connectivity (FC)*

Functional MRI (fMRI) allows for approximate mappings of brain activity through Blood-oxygen-level-dependent (BOLD) imaging, which exploits neurovascular coupling-based increased perfusion in active brain regions as a surrogate measure of neuronal activation that has good spatial resolution and is non-invasive (17,18). Functional activation studies have recapitulated previously known relationships between brain anatomy and function, regarding sensory (19,20), motor (21,22) and higher-order cognitive functions such as attention(23), cognitive control (24), memory (25), and social cognition (26). Furthermore, fMRI enables the study of the novel anatomical mode of functional connectivity (FC). FC establishes relationships between brain areas based on correlations in their time-course of activations, describing “*temporal correlations between remote neurophysiological events*” (27). Importantly, FC does not establish a causal relationship between regional activity patterns.

Through FC, it is possible to discover networks of functional co-activations, both using task paradigms (28), as well as in fMRI scans performed in resting state, yielding intrinsic organizational networks. Notable FC-derived cartographies include the Yeo-Krienen networks of the cerebral cortex (29) or the Buckner networks of the cerebellar cortex (30). These functional cartographies derived from resting-state FC distinguish themselves from classical cytoarchitectonic mapping by establishing spatially discontinuous intercortical relationships, as can be exemplified by the Default Mode Network (31). As such, FC-derived cartography is important in developing a network-like understanding of human brain architecture which focuses on understanding cognitive processes as resulting from interactions between brain regions, rather than having a single anatomical location that is uniquely responsible for them - a view was already popularized by Brodmann.

#### *Structural Connectivity (SC)*

White matter tracts serve as physical information highways between different brain regions, and rich knowledge about axonal connections in animals could be derived via tract-tracing studies (32). As these are not possible in live humans, here, diffusion MRI (dMRI)-based tractography, the probabilistic reconstruction of white matter tracts through diffusivity

measurements, can be used to study the white matter connections in the human brain. Structural connectivity (SC) is the measure of inter-areal connectedness by fiber tracks and, analogously to FC, enables a novel neuroanatomical perspective. Especially graph-theoretical studies of SC networks revealed interesting insights about the organization of white matter connections. One striking organizational propensity of macro- and micro-scale structural networks is their small-world architecture (33), which is characterized by short path lengths and high clustering (34), with sub-network clusters communicating with each other through high-degree hub nodes. Hub nodes strongly interconnected amongst each other form the so-called rich club (35). Disturbance in hub node architectures has been found in patients with schizophrenia, suggesting illness-associated alterations in structural connectomes (36). Importantly, hub nodes are also found in FC-derived networks, and their locations overlap with SC-derived network hubs (37). Although an intuitive proposition would be that structural and functional connectivity should generally overlap, as they can be thought to represent “two sides of the same coin”, correlation strengths between these measures realistically do not exceed  $r \sim 0.5$  (2). Therefore, even with these measures, it is still an ongoing challenge to connect the structural and functional anatomy of the brain.

### **1.1.3 Other brain mapping efforts**

#### *Cortical thickness variation*

The thickness of the cerebral cortex is not uniform throughout the brain. Cortical thickness can be measured *in vivo* via cranial MRI and varies inter-individually, developmentally, and in a normative topographical fashion (38,39). As systematical cortical thickness alterations can be associated with psychiatric and neurological illnesses, it can furthermore be used as a proxy to study disease-associated morphological changes. As large sample sizes are needed to assess disease-associated variations in cortical thickness with sufficient statistical power, the most relevant advances have been made by the Enhancing NeuroImaging Genetics through Meta-Analysis (ENIGMA) consortium (40), a large-scale, multi-site effort that collected data from over thousands of patients and controls per disease to quantify disease-associated cortical thickness alterations in multiple neurological and psychiatric diseases such as epilepsy (41), major depressive disorder (42) and schizophrenia (43). Since cortical

thickness constitutes a proxy measure for structural cortical characteristics, such as cytoarchitectonic properties and neuronal density (44–46), neurobiologically meaningful interpretations of cortical thickness alterations are possible. The ENIGMA consortium has therefore expanded brain mapping into the pathological domain.

### *fMRI-based meta-analytical approaches*

The mapping of functional brain organization using fMRI has also been realized through approaches other than FC. Leveraging standardized coordinate spaces used in MRI studies, functional activations can be summarized across multiple studies, yielding probabilistic meta-analytical activation maps derived from large sample sizes (47). Furthermore, meta-analytical approaches can - rather than imbuing brain cartography data with functionally meaningful interpretations as the previously described brain mapping approaches - generate cartography data tailored to specific neurocognitive functions. Here, a prominent effort that combines text-mining and meta-analytical activation maps to generate term-based maps of functional brain activation is the neurosynth study (48). Briefly summarized, text-mining selects terms of interest used with a high frequency across manuscripts, subsequently extracts fMRI-based functional activation coordinates from the corresponding studies and associates these activations with the selected terms of interest. Expanding further on the term-based approach, terms can be algorithmically summarized into functionally contingent topics, performing a functionality-based dimensionality reduction of the often not ontologically soundly defined terms used in cognitive neuroscience (49,50). Neurosynth's automated approach can generate meta-analytical functional activation maps from a large sample size without the need for human supervision. Drawing on the strengths of standardized coordinate spaces to increase sample size, meta-analytical approaches are powerful tools in understanding regional functional specializations in the human brain.

## 1.2 Neurotransmitter systems in the human brain

The previous section outlined how different cartographical approaches contributed to our understanding of the human brain. The current study introduces a novel anatomical perspective based on the brain's chemoarchitecture, a structural component with important ties to cytoarchitectural characteristics and functional anatomy.

### 1.2.1 Neurotransmitter mapping

Similar to other structural features of brain organization, neurotransmitter receptor expression has been systematically mapped in the human brain. Receptor autoradiography studies, which perform accurate and specific mapping of different neurotransmitter receptor distributions in *post-mortem* brain slices, have shown that receptor distributions vary distinctly throughout the cerebral cortex. For example, visual cortex has high GABA<sub>A</sub> receptor density, while no  $\mu$ -opioid receptors are found there (51,52). Receptor expression patterns show similarities with cytoarchitectural characteristics. Horizontally, receptor distributions vary in a laminar fashion, partially overlapping (53,54) with cytoarchitectural cortical layers, where the granularity of a cortical layer is an important determinant of receptor density profiles (55). Similarly, receptor co-distributions vary largely as a function of cytoarchitecturally-defined cortical areas, but can both group different histologically-defined areas into neurochemical families or perform further subdivision of regions that show a homogeneous cytoarchitectural profile (54,56). Here, the subdivision of Broca's region by distinct neurochemical profiles is an impressive example (57).

Autoradiographic mapping of neurotransmitter receptors enables detailed assessments of regional chemoarchitectural characteristics. However, the approach is resource-heavy and relies on *ex-vivo* tissue. A complementary technique is Positron Emission Tomography (PET)-based receptor mapping. Here, neurotransmitter receptors are targeted with specific radioligands in live humans, which allows for the reconstruction of a whole-brain profile of receptor densities, trading resolution for scalability to larger cohorts and *in-vivo* measurements. *In-vivo* imaging enables the study of receptor distributions in pathological conditions, with scintigraphic assessment of cerebral DAT density in diagnosing Parkinson's disease being a practical example. Furthermore, neurotransmitter receptor and transporter distributions have been studied with PET imaging in brain mapping efforts (58,59).

### **1.2.2 Functional relevance of neurotransmission and neurotransmitter mapping**

Autoradiography studies have established that changes in localized brain function and changes in receptor distributions coincide, as can be exemplified in the visual cortex (51,60). Measuring multiple receptor densities in the same brain area allows for the creation of receptor “fingerprints” – multidimensional chemoarchitectural profiles that are important features of functional specialization (54,60–62). As such, receptor fingerprints in motor areas markedly differ from those in sensory areas (63), and delineate primary from association cortices in multiple modalities of analysis (64,65). Consistently, areas of similar functionality also show similarities in receptor fingerprints. For example, areas involved in language comprehension share a chemoarchitectural basis (66), and resting-state FC networks show increased homogeneity in receptor fingerprints (67). Functionally, pharmacological manipulations of neurotransmitter systems induce changes in FC. For example, subjects treated with atomoxetine showed increased functional network segregation (68), and sulpiride treatment led to impaired global and local efficiency of FC networks (69). Furthermore, LSD-induced 5-HT<sub>2a</sub> agonism increased global connectivity of association cortices (70), and psilocybin-induced 5-HT<sub>2a</sub> stimulation increased global FC network integration (71). Importantly, the changes in functional connectivity measures were most pronounced in brain areas with high expression of 5-HT<sub>2a</sub>, clearly associating the underlying receptor architecture with functional changes. Combined, these findings add to the hypothesis that neuromodulation via neurotransmission is a “missing link” in brain structure-function relationships, as disparities between structural and functional connectivity patterns (2,72) prompted the search for novel determinants of inter-areal functional relationships. Especially the pharmacological intervention studies suggest that neuromodulation could be a key component in understanding how a static physical wiring structure gives rise to flexible functionality. Therefore, a deeper understanding of how the neurotransmitter landscape is organized could help bridging the gap that still stands between structural and functional anatomy of the brain.

### **1.2.3 Relevance of neurotransmitter systems in clinical medicine**

Finally, the vast majority of psychotropic drugs interact with the cerebral neurotransmission landscape, but there is no general rule that links a neurotransmitter system to a clear cognitive function. One important determinant is the receptor type a neurotransmitter binds to, exemplified by how 5-HT1a and 5-HT2a receptors differentially contribute to coping in stressful situations (73). However, translating biochemical differences occurring after receptor binding into a mechanistic explanation for their differential contribution to coping has not been possible. Furthermore, receptor topography and organization into different pathways also influences receptor-mediated functions. For example, the dopamine system segregates into multiple well-studied pathways. The nigro-striatal pathway is essential for motor functions, the tubero-infundibular pathway regulates synthesis of prolactin, and the meso-limbic as well as meso-cortical pathways are involved in higher cognitive functions, such as reward processing and cognitive control. Their shared receptor architecture is of utmost clinical relevance, as drugs targeting the dopamine system can affect each of these pathways, leading to medication side effects. As such, antipsychotic treatment with D2 antagonists can lead to extrapyramidal motor symptoms through affecting the nigro-striatal pathway, and to hyperprolactinemia through affecting the tubero-infundibular pathway. A better understanding of chemoarchitectural anatomy could therefore also hold direct clinical implications.

### **1.3 Aims of this work**

This study aims at a characterization of cortical and subcortical chemoarchitectural anatomy. A large open-access dataset of PET-derived NTRM density maps, consisting of 19 different NTRM distributions collected across more than 1200 subjects is used as the primary resource. To generate a chemoarchitecturally-based cartography, brain regions are studied with respect to their interregional chemoarchitectural similarity, as measured by a covariance matrix termed the “receptome”. Following, principal gradient decomposition, a non-linear dimensionality reduction method, identifies the main axes of chemoarchitectural similarity. These axes provide novel perspectives on intercortical as well as intersubcortical

relationships and are subsequently employed to generate an overview over general principles of the receptome. NTRM co-distribution patterns that drive cortical and subcortical chemoarchitectural similarity are analyzed. Furthermore, the spatial patterns of gradients can be put in context with multiple other neuroanatomical modes to gain a deeper understanding of features that unify as well as differentiate chemoarchitectural anatomy and other neuroanatomical modes. This work draws on other brain mapping techniques outlined in the first chapter, comparing chemoarchitectural similarity to functional and structural connectivity as well as cytoarchitectural characteristics. To gain a functional understanding, receptome gradients are compared to meta-analytical brain activation maps, allowing for a perspective on functional and chemoarchitectural co-differentiation patterns. Similarly, through comparing disease-associated cortical thinning maps to receptome gradients, associations between chemoarchitectural anatomy and central nervous system diseases are investigated. Additionally, node-level clustering analyses of cytoarchitectural similarity aim at delineating receptome-driven communities in the cortex, which are compared to functionally as well as cytoarchitecturally-derived communities. Finally, next to the cerebral cortex, subcortical nuclei are investigated with regards to their chemoarchitecture, taking first steps towards an understanding of the comparatively understudied chemoarchitecture of the subcortex.

This study solely re-analyses previously published data from various datasets that have already received ethics approval from their respective institutions. Therefore, this study is performed within the scope of the vote to study number 2018-317 issued on 30.10.2021 by the Ethics Committee at the Faculty of Medicine at Heinrich Heine University Düsseldorf to Prof. Dr. Simon Eickhoff. No animal experiments are performed.

- 2 **Publication:** Hänisch B., Hansen J.Y., Bernhardt B.C., Eickhoff S.B., Dukart J., Misić B., Valk S.L.: Cerebral chemoarchitecture shares organizational traits with brain structure and function; eLife (2023)

\*For correspondence: [s.valk@fz-juelich.de](mailto:s.valk@fz-juelich.de)

**Competing interest:** The authors declare that no competing interests exist.

**Funding:** [See page 17](#)

**Preprinted:** [26 August 2022](#)

**Received:** 30 September 2022

**Accepted:** 12 July 2023 **Published:** 13 July 2023

**Reviewing Editor:** Birte U Forstmann, University of Amsterdam, Netherlands

© Copyright Hänisch *et al.* This article is distributed under the terms of the [Creative Commons Attribution License](#), which permits unrestricted use and redistribution provided that the original author and source are credited.

RESEARCH ARTICLE

# Cerebral chemoarchitecture shares organizational traits with brain structure and function

Benjamin Hänisch<sup>1,2,3</sup>, Justine Y Hansen<sup>4</sup>, Boris C Bernhardt<sup>4</sup>, Simon B Eickhoff<sup>1,2</sup>, Juergen Dukart<sup>1,2</sup>, Bratislav Misic<sup>4</sup>, Sofie Louise Valk<sup>1,2,3\*</sup>

<sup>1</sup>Institute of Neuroscience and Medicine, Brain and Behaviour, Research Centre Jülich, Jülich, Germany; <sup>2</sup>Institute of Systems Neuroscience, Medical Faculty, Heinrich Heine University Düsseldorf, Düsseldorf, Germany; <sup>3</sup>Otto Hahn Group Cognitive Neurogenetics, Max Planck Institute for Human Cognitive and Brain Sciences, Leipzig, Germany; <sup>4</sup>McConnell Brain Imaging Centre, Montréal Neurological Institute, McGill University, Montréal, Canada

---

**Abstract** Chemoarchitecture, the heterogeneous distribution of neurotransmitter transporter and receptor molecules, is a relevant component of structure–function relationships in the human brain. Here, we studied the organization of the receptome, a measure of interareal chemoarchitectural similarity, derived from positron-emission tomography imaging studies of 19 different neurotransmitter transporters and receptors. Nonlinear dimensionality reduction revealed three main spatial gradients of cortical chemoarchitectural similarity – a centro-temporal gradient, an occipito-frontal gradient, and a temporo-occipital gradient. In subcortical nuclei, chemoarchitectural similarity distinguished functional communities and delineated a striato-thalamic axis. Overall, the cortical receptome shared key organizational traits with functional and structural brain anatomy, with node-level correspondence to functional, microstructural, and diffusion MRI-based measures decreasing along a primary-to-transmodal axis. Relative to primary and paralimbic regions, unimodal and heteromodal regions showed higher receptomic diversification, possibly supporting functional flexibility.

---

### Editor's evaluation

This work provides a valuable structural and functional characterization of the neurotransmitter's spatial distribution heterogeneity in cortical and subcortical regions. The authors report a systematic description and annotation of a new 'layer' of brain organization that has been relatively poorly integrated with the wider neuroimaging literature to date. In sum, this article has the potential to be of great interest to a wide audience in neurosciences.

---

### Introduction

Uncovering how the anatomy of the human brain supports its function is a long-standing goal of neuroscientific research (*Suárez et al., 2020*). Histological mapping studies found that brain areas vary substantially in cellular composition and established a link between cytoarchitectural and functional diversity (*Brodmann, 1909; von Koskinas and Koskinas, 1925; Vogt and Vogt, 1919*). Next to cellular composition, the brain's chemoarchitecture, the distribution of neurotransmitter receptor and transporter molecules (NTRM) across the cortical mantle, is a similarly important mode of brain neurobiology. Neurotransmitter receptors show a heterogeneous distribution throughout the cortex, closely related to both vertical (laminar) and horizontal cyto- and myeloarchitectural composition,

as shown using postmortem autoradiographical receptor labeling (*Eickhoff et al., 2007; Zilles and Amunts, 2009*). Receptor distributions recapitulate histology- defined cortical areas, but also organize different cortical areas into neurochemical families and further subdivide homogeneous cytoarchitectural regions (*Zilles and Amunts, 2009; Zilles and Palomero- Gallagher, 2001*). Changes in localized brain function are reflected by changes in receptor distributions, as demonstrated in the changes of multiple receptor densities at the border between primary (V1) and secondary (V2) visual cortex (*Eickhoff et al., 2008; Zilles et al., 2004*). Crucially, brain areas sharing similar functionalities also display similarities in the density profiles of multiple neurotransmitter receptor types, the so-called receptor ‘fingerprint’ (*Zilles and Amunts, 2009; Zilles et al., 2004; Zilles et al., 2002; Morosan et al., 2005*). For example, receptor fingerprints delineate sensory from association cortices (*Dehaene et al., 2005*) and provide a common molecular basis of areas involved in language comprehension (*Zilles et al., 2015*), strongly indicating receptor fingerprints as key features supporting functional specialization. Therefore, dissecting the brain’s chemoarchitectural landscape could be crucial in understanding structure–function links in the human brain. Comprehensive analysis of receptor fingerprints has mostly been limited to autoradiography experiments in postmortem brain slices. Recently, multisite efforts agglomerated large- scale open- access datasets of whole- brain NTRM density distributions derived from positron- emission tomography studies, enabling the in vivo study of chemoarchitecture (*Hansen et al., 2022; Dukart et al., 2021*). Using this resource, Hansen et al. delineated associations between NTRM density profiles and oscillatory neural dynamics, meta-analytical studies of functional activation, as well as disease- associated cortical abnormality maps. Importantly, they showed that brain regions in the same resting-state functional connectivity (FC) networks as well as structurally connected brain regions display increased chemoarchitectural similarities (*Hansen et al., 2022*), replicating structure–function relationships evident from autoradiography studies (*Zilles and Amunts, 2009*).

These findings, along with the implications of receptor fingerprints in functional specialization, warrant the study of whole- brain, in vivo imaging-derived chemoarchitectural anatomy of the brain. An improved understanding of organizational principles of the neurotransmission landscape could prove critical for basic neuroscience, but also benefit clinical medicine. NTRMs are highly relevant in mental health care, as an extensive body of research links alterations in NTRM expression and distribution patterns to

psychiatric diseases (*Nautiyal and Hen, 2017; Seeman, 2013; Quah et al., 2020; Lydiard, 2003*). Additionally, most psychotropic drugs manipulate the brain's neurotransmission landscape and are effective and reliable pillars in the treatment of psychiatric diseases (*Cipriani et al., 2018; Huhn et al., 2019; Soomro et al., 2008; Geddes and Miklowitz, 2013*), although their mechanisms of action are often incompletely understood. Complementary, clinical phenotypes are associated with alterations in multiple neurotransmitter systems (*Moncrieff et al., 2022; Kaltenboeck and Harmer, 2018; Kesby et al., 2018*). Characterizing the spatial organization of chemoarchitectural features could therefore provide novel avenues toward understanding the neurobiology of psychiatric diseases (*Dean and Keshavan, 2017; Harrison et al., 2018; Luvsannyam et al., 2022; Pauls et al., 2014*).

We furthermore aim to study the anatomy of subcortical chemoarchitecture as the question stands if the relationship between receptor fingerprints and functional specialization observed in the cortex could be generalized to subcortical nuclei (*Zilles and Amunts, 2009; Zilles et al., 2015*). Since cortical disparities between functional and structural connectivity could be partly explained by subcortical ascending neuromodulatory projections (*Bell and Shine, 2016; Shine, 2019*), a clearer understanding of subcortical chemoarchitecture and its relationship to cortical chemoarchitecture could provide a novel perspective on whole- brain structure–function relationships (*Forstmann et al., 2017*).

Here, we leverage the aforementioned resource published by Hansen et al. to generate and characterize the 'receptome,' a neuroanatomical measure that reflects the interregional similarities of brain regions based on their NTRM fingerprints. To study the spatial organization of chemoarchitectural similarity, we employ an unsupervised dimensionality reduction technique to generate principal gradients, which are low- dimensional representations of the organizational axes in the cortical and subcortical receptome. Using these gradients, we identify NTRM distributions that drive regional receptor (dis)similarity. Several follow- up analyses shed light upon the relationship to organizational axes in structural connectivity (SC), as measured using diffusion MRI (*Yeh et al., 2021*), microstructural profile covariance (MPC) (*Paquola et al., 2019*), and resting- state functional connectivity (rsFC) (*Logothetis, 2008*). Finally, we performed meta- analytic decoding of chemoarchitectural gradients to assess their relations to topic- based functional brain activation (*Yarkoni et al., 2011*) and investigated their relationship to radiological markers of disease (*Thompson et al., 2014*). We

performed various analyses to evaluate the robustness of our observations.

## Results

### Organization of the cortical receptome (Figure 1)

To assess cortical chemoarchitecture, we leveraged a large publicly available dataset of PET- derived NTRM densities, containing 19 different NTRM from a total of over 1200 subjects (*Hansen et al., 2022*). After parcellating the receptor maps into 100 parcels according to the Schaefer atlas (*Schaefer et al., 2018*), we calculated a Spearman rank correlation matrix of parcel- level NTRM densities, the receptome. The receptome represents node- level interregional similarities in NTRM fingerprints. Next, we employed nonlinear dimensionality reduction techniques by leveraging diffusion map embedding to delineate the main organizational axes of cortical chemoarchitectural similarity. A schematic introducing the different NTRM and the workflow is outlined in *Figure 1A*. See Table S1 for a detailed overview of the PET NTRM density maps.

Diffusion embedding- derived gradients showed high correspondence to axes derived by linear dimensionality reduction techniques (*Figure 1—figure supplement 1A*). The first 11 components explained significantly more variance compared to gradients decomposed from receptomes generated from randomized NTRM density maps (*Figure 1—figure supplement 1B*). We chose to focus on the first three gradients, which explained 15, 14, and 13% of relative variance, respectively, due to a marked drop in variance explained after these three components (*Figure 1A*). The first receptome gradient (RC G1) described an axis stretching between somato- motor regions and inferior temporal and occipital lobe. The second receptome gradient (RC G2) spanned between a temporo- occipital and a frontal anchor. Finally, the third receptome gradient (RC G3) was differentiated between the occipital cortex and the temporal lobe (*Figure 1B*).

To determine which NTRM distributions drive the main axes of cortical chemoarchitectural similarity, we performed Spearman rank correlations between a parcel's associated gradient value and its NTRM fingerprint, meaning density profiles of all NTRM in that parcel (*Figure 1C*). Note that the gradient value of a parcel is a measure of where on the gradient axis the parcel is located, from which similarity to parcels with similar values, and dissimilarity to parcels with dissimilar values, is inferred. Thus, a receptor with higher density in parcels with negative values and lower density in parcels

with positive values will be negatively correlated to the gradient. RC G1 was primarily driven by the anticorrelation between distributions of 5-HTT, 5-HT4, 5-HT2a, and GABA<sub>A</sub> with the distributions of VAcHT, H3, NAT, and A4B2. RC G2 separated 5-HTT, DAT, NMDA, D1, and GABA distributions from  $\alpha4\beta2$ , 5-HT1b, CB1, H3, and MU. RC G3 showed significant negative correlations to GABA<sub>A</sub> distributions and significant positive correlations to D1, 5-HT1a, CB1, MU, 5-HT4, and VAcHT.

### **Organization of the subcortical receptome (Figure 2)**

Following our analysis of cortical NTRM similarity, we investigated the chemoarchitecture of subcortical nuclei. We selected the caudate nucleus, putamen, nucleus accumbens, pallidal globe, thalamus, and amygdala as regions of interest (ROIs). To gain an understanding of how different the cerebral cortex and subcortical nuclei are in their chemoarchitectural composition, we performed a multidimensional scaling projection of cortical and subcortical NTRM density profiles that were z-scored across both compartments (*Figure 2—figure supplement 1A*). Subcortical nuclei were shown to be largely separate from cortical structures, with the exception of amygdala. NTRM density profiles z-scored only within subcortical nuclei were used in subsequent analyses.

First, to investigate whether NTRM fingerprints in subcortical nuclei were associated with functional specialization, as observed in cortical areas, we performed agglomerative hierarchical clustering on the z-scored mean NTRM density profiles of subcortical ROIs per hemisphere (*Figure 2A*). Subcortical chemoarchitecture was largely symmetrical between hemispheres, as indicated by the immediate clustering of structures with their counterpart from the other hemisphere. The main hierarchical branch separated putamen, accumbens nucleus, caudate nucleus (the striatum), and pallidum from amygdala and thalamus. Thalamus and striatum had considerable differences in NTRM co-expression patterns.  $\alpha4\beta2$ , NAT, 5-HTT, and NMDA showed strong co-expression in thalamus but not in striatum,

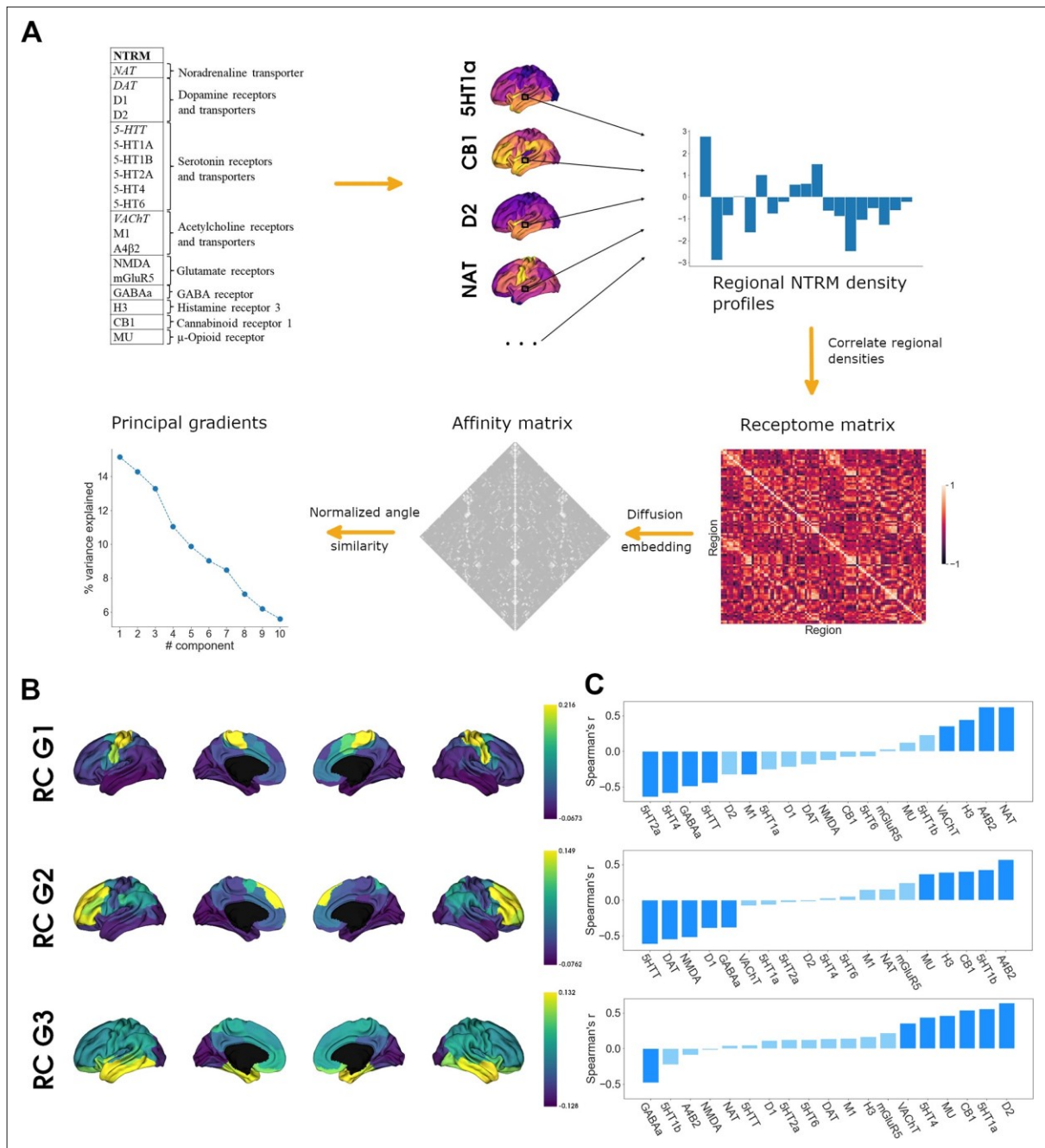


**Figure 1.** Organization of the cortical receptome. **(A)** Analytic workflow of receptome generation and gradient decomposition. Node-level neurotransmitter receptor and transporter molecule (NTRM) fingerprints are derived from PET images of 19 different NTRM (in the top left, italic font denotes transporters). The fingerprints are then Spearman rank correlated to capture node-level similarity in chemoarchitectural composition, generating the receptome matrix. Next, to determine similarity between all rows of the receptome matrix, we used a normalized angle similarity kernel to generate an affinity matrix. Finally, we employ diffusion embedding, a nonlinear dimensionality reduction technique, to derive gradients of receptomic organization. **(B)** Receptome (RC) gradients projected on the cortical surface. Top: first receptome gradient (RC G1); middle: second receptome gradient (RC G2); bottom: third receptome gradient (RC G3). **(C)** Spearman rank correlations of cortical receptome gradients with individual NTRM densities. Top: first receptome gradient; middle: second receptome gradient; bottom: third receptome gradient. Saturated blue coloring corresponds to statistically significant correlations at  $p < 0.05$ .

The online version of this article includes the following figure supplement(s) for figure 1:

**Figure supplement 1.** Cortical receptome gradients.

**Figure supplement 2. Robustness of receptome gradients.**

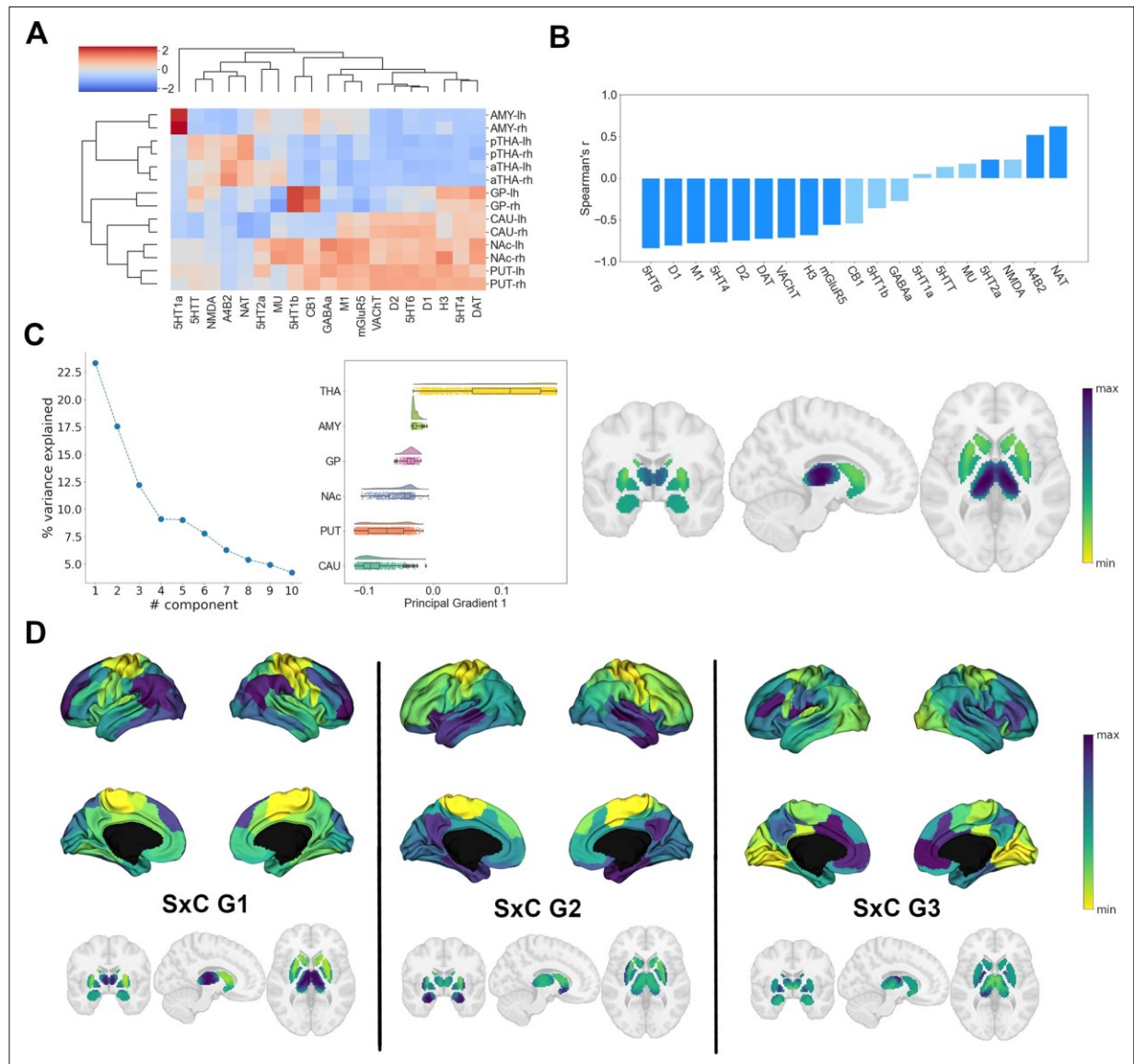


**Figure 2.** Organization of subcortical chemoarchitecture. **(A)** Hierarchical agglomerative clustering of neurotransmitter receptor and transporter molecule (NTRM) densities in subcortical structures. aTHA: anterior thalamus; pTHA: posterior thalamus. **(B)** Spearman rank correlations of the first subcortical receptome gradient with individual NTRM densities. Saturated blue coloring corresponds to statistically significant correlations at  $p < 0.05$ .

**(C)** Gradient decomposition of the subcortical receptome. Left: percentage of variance explained by components following gradient decomposition.

Middle: value distribution of the first subcortical receptome gradient across subcortical structures. CAU: caudate nucleus; PUT: putamen; NAc:

accumbens nucleus; GP: pallidal globe; AMY: amygdala; THA: thalamus. Right: subcortical projection of the first subcortical receptome gradient. **(D)** Gradients of the subcortico-cortical receptome projected to the cortical surface and to subcortical nuclei.

The online version of this article includes the following figure supplement(s) for figure 2:

**Figure supplement 1.** Subcortical receptome.

**Figure supplement 2.** Robustness of agglomerative hierarchical clustering – subcortex.

while D1, D2, DAT, 5-HT<sub>4</sub>, 5-HT<sub>6</sub>, M1, and VACHT were strongly co-expressed in striatum, but not in thalamus.

Then, we analyzed chemoarchitectural similarity in subcortical nuclei through constructing a receptome by voxel-wise Spearman rank correlations of NTRM density profiles in the subcortical ROIs. To discern how subcortical nuclei can be reconstructed based on chemoarchitectural similarity, we employed the Leiden community detection method (*Traag et al., 2019*), a greedy optimization algorithm that opts to minimize variance within and maximize variance between communities.

Subcortical receptome clustering exhibited high stability across the resolution parameter sample space (*Figure 2—figure supplement 1A*). Receptomic clustering discerned three dominant communities, the first mainly capturing the striatal structures (putamen, caudate, NAc) and the pallidal globe, the second mainly capturing the thalamus, and the third mainly capturing the amygdala (*Figure 2—figure supplement 1A*). We then used diffusion embedding to derive low-dimensional gradient embeddings of the subcortical receptome to discern its main organizational axes. The first subcortical receptome gradient (sRC G1), explaining 23% of relative variance, was anchored between the striatum and the thalamus (*Figure 2C*). Note that proximity of structures was not a major determinant of sRC G1 values, demonstrated by voxels of the caudate nucleus and thalamus that were proximal to each other but showed diverging sRC G1 values. The second gradient, explaining 17.5% of relative variance, and third gradient, explaining 12% of relative variance, described ventral-dorsal and medial-lateral trajectories, respectively (*Figure 2—figure supplement 1*). The first subcortical receptome gradient showed significant positive correlations to NAT,  $\alpha$ 4 $\beta$ 2, and 5-HT<sub>2a</sub> densities, and significant negative correlations to 5-HT<sub>6</sub>, D1, M1, 5-HT<sub>4</sub>, D2, DAT, VACHT, H3, and mGluR5 distributions (*Figure 2B*).

Lastly, we were interested in the relationship between the subcortical and cortical receptomes. We created a subcortico-cortical NTRM covariance matrix and applied diffusion embedding to delineate the gradients of subcortico-cortical chemoarchitectural similarity (*Figure 2D*). The first and second cortical gradients correlated significantly with all subcortico-cortical receptome gradients, while the third cortical gradient only correlated significantly to the third subcortico-cortical gradient (*Figure 2—figure supplement 1D*).

### **Relationship of the cortical receptome to brain functional processing and disease (Figure 3)**

After characterizing the cortical and subcortical receptomes, we sought to investigate the relationship of chemoarchitectural similarity to hallmarks of brain functional processing and dysfunction. To assess brain functional processing, we used topic-based meta-analytical maps of task-based functional brain activation. This approach associates data-driven semantic topics with localized brain activity (e.g. 'primary somatomotor' is associated with activation in the precentral gyrus). Using the Neurosynth database (*Yarkoni et al., 2011*), we calculated Spearman rank correlations between normalized activation maps and receptome gradients while accounting for spatial autocorrelation (*Figure 3B*). Negative correlations imply a relationship between topic-based functional activations mainly located in parcels with negative gradient values. RC G1 showed strong positive correlations with meta-analytical topics of sensory-motor function (topics 2, 17, and 32) and control (topics 16 and 20). Its strongest negative correlations were to topics capturing facial and emotion recognition (topic 40) as well as categorizing and abstract functions (topic 38). RC G2 displayed positive correlations to topics of control (topics 16, 20, and 48) and memory (topic 9), differentiating them from topics of facial and emotion recognition (topic 40) and categorizing and abstract functions (topic 38), with which it showed negative correlations. Lastly, RC G3 showed positive correlations of note to topics related to language and speech (topics 6 and 46) compared to negative correlations to topics of attention and task performance (topics 15 and 47), memory (topic 9), and mental imagery (topic 41).

Secondly, we investigated the association between chemoarchitectural organization and neurodevelopmental conditions or disorders. We leveraged disease-related cortical thickness alterations, a radiological marker of structural abnormalities, derived via a standardized multisite effort (*Thompson et al., 2014*). Cortical thickness was quantified by Cohen's *d* case-v.s.-control effect size and accessed through the ENIGMA toolbox (*Larivière et al., 2021*). We selected autism spectrum disorder (ASD) (*van Rooij et al., 2018*), attention-deficit hyperactivity disorder (ADHD) (*Hoogman et al., 2019*), bipolar disorder (BPD) (*Hibar et al., 2018*), DiGeorge syndrome (22q11.2 deletion syndrome) (DGS) (*Sun et al., 2020*), epilepsy (EPS) (*Whelan et al., 2018*), major depressive disorder (MDD) (*Schmaal et al., 2017*), obsessive compulsive disorder (OCD) (*Boedhoe et al., 2018*), and schizophrenia (SCZ) (*van Erp et al., 2018*) to cover a broad spectrum of diseases (*Figure 3C*).

Receptome gradients captured disease- specific cortical thickness alteration patterns. RC G1 showed positive correlations to the cortical thickness profile of OCD, while RC G2 had negative correlations to cortical thickness alterations in BPD. Both OCD and BPD were primarily associated with cortical thinning, thus, cortical thickness in OCD was reduced where RC G1 values were positive,

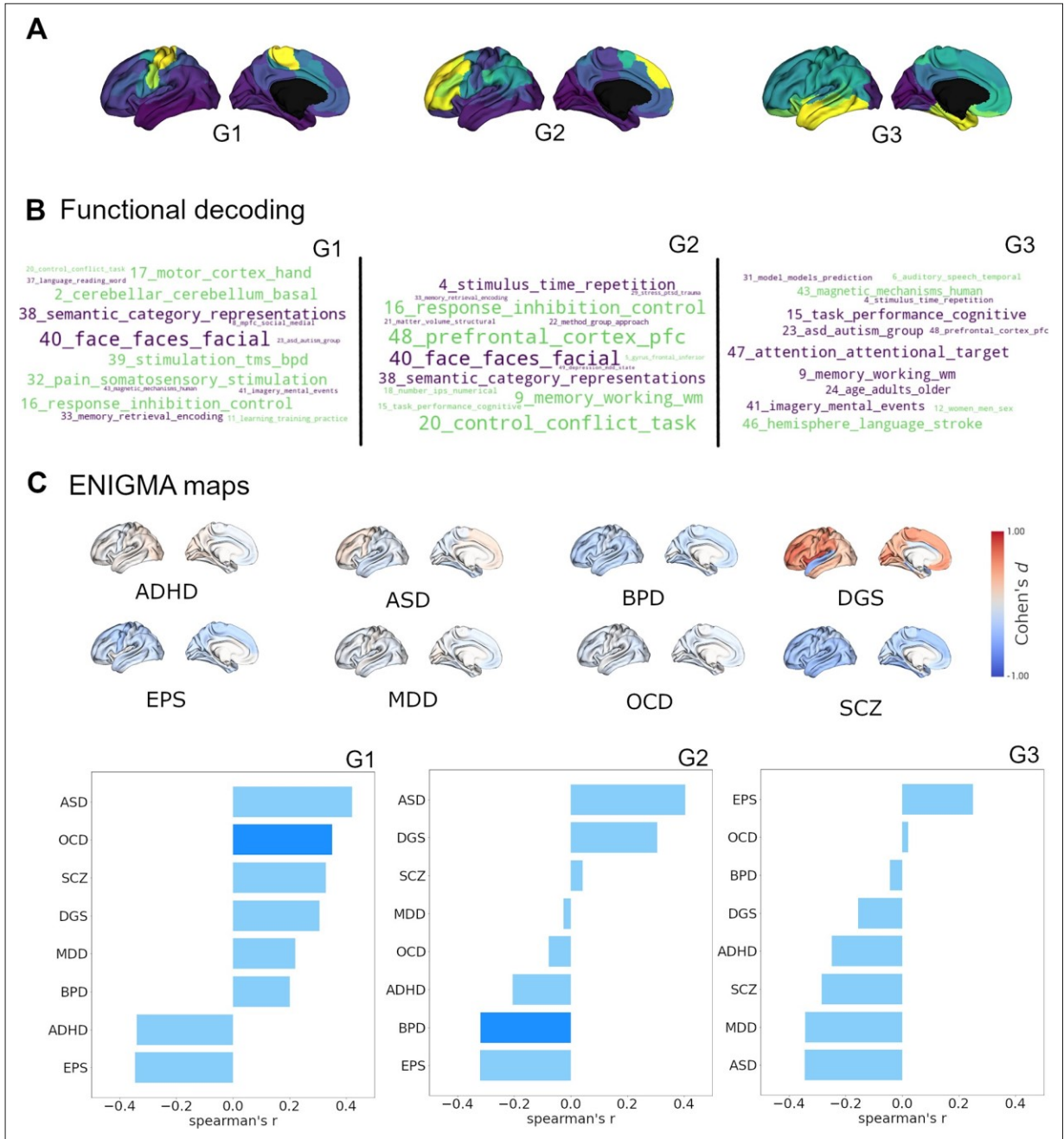


**Figure 3.** Cortical receptome gradients in term-b ased functional activation and disorder. **(A)** Cortical receptome gradients projected to the cortical surface. **(B)** Functional decoding of cortical receptome gradients. Wordclouds display positive and negative correlations of receptome gradients and topic- based functional activation patterns. Word sizes encode absolute correlation strength, word colors are matched to the respective gradient poles. Only statistically significant correlations ( $p < 0.05$ ) are displayed. Left: RC G1; middle: RC G2; right: RC G3. **(C)** Disease decoding of cortical receptome gradients. Surface plots: effect size (Cohen's *d*) of cortical thickness alterations

in central nervous system disorders in patients vs. controls. Bar plots: Spearman rank correlations of receptome gradients and cortical thickness alterations. Saturated blue coloring corresponds to statistically significant correlations at  $p < 0.05$ . Left: RC G1; middle: RC G2; right: RC G3.

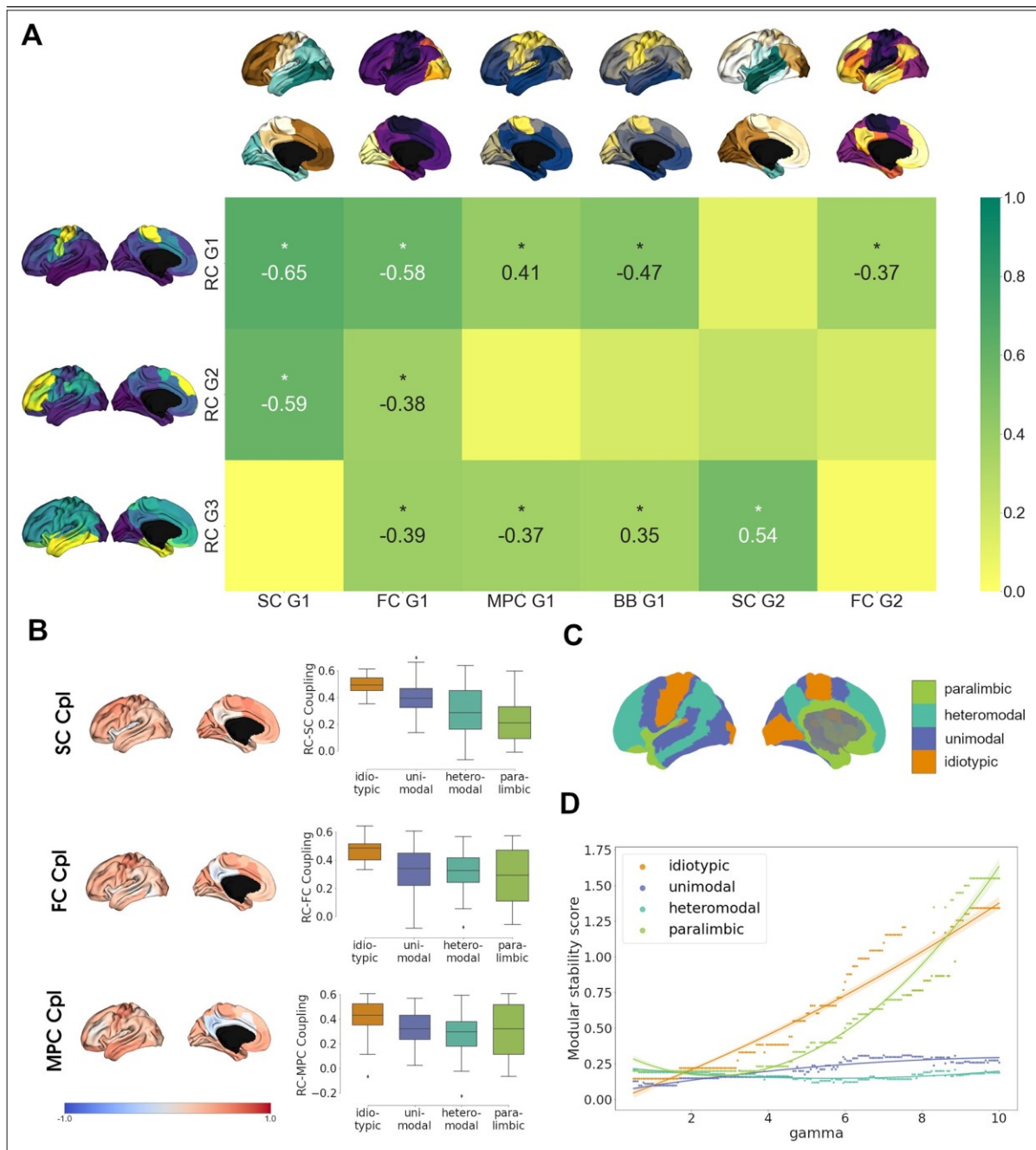


**Figure 4.** Multimodal contextualization of the cortical receptome. **(A)** Correlation strengths of cortical receptome gradients to functional connectivity (FC), structural connectivity (SC), microstructural profile covariance (MPC), and BigBrain gradients. Coloring is scaled to absolute values. Surface-projected gradients are displayed next to their respective rows and columns. Asterisks indicate statistically significant correlations at  $p < 0.05$ . **(B)** Coupling of the cortical receptome to SC, FC, and MPC. Left: surface projection of coupling strengths. Right: coupling strengths across cytoarchitectural classes. **(C)** Surface projection of Mesulam cytoarchitectural classes. **(D)** Modular stability of receptome clustering in Mesulam cytoarchitectural classes, reflecting the heterogeneity of receptomic profile.

The online version of this article includes the following figure supplement(s) for figure 4:

**Figure supplement 1.** Contextualization of receptome gradients in hierarchical brain organization. **Figure supplement 2.** Robustness of agglomerative hierarchical clustering – cortex.

and BPD- associated reductions in cortical thickness were located where RC G2 values were negative. RC G3 did not show significant associations with cortical disease profiles. (*Figure 3C*).

### **Interrelationship between the cortical receptome and structural, functional, and cytoarchitectural organization (Figure 4)**

Finally, we investigated the relationship of cortical chemoarchitectural similarity to other measures of cortical organization. We first analyzed whether functional brain networks (*Thomas Yeo et al., 2011*) significantly aligned along receptome gradients by comparing gradient value distributions inside functional networks against 1000 random gradient maps generated via variogram matching (*Figure 4— figure supplement 1*). RC G1 showed alignment to the somato- motor network that forms its positive anchor. RC G2 was aligned to default mode and control networks, which are located in the positively anchoring regions, and the visual network, which is located on the opposite side of the gradient. Lastly, RC G3 was aligned with limbic and visual networks, which are located at opposite poles of the gradient.

Then, we aimed to perform a broad multimodal contextualization of cortical chemoarchitectural anatomy. As autoradiography studies connect receptor distributions to cytoarchitectural characteristics (*Zilles and Amunts, 2009*), we compared cortical receptomic organization to MPC, an MRI- derived proxy measure of cortical microstructure (*Foit et al., 2022*), and a gradient of cytoarchitectural variation from the BigBrain project (*Paquola et al., 2019; Amunts et al., 2013*) (BB G1). Additionally, we explored the relationships of cortical chemoarchitectural similarity to diffusion MRI tractography-derived SC, and functional MRI- derived resting-state FC, as previous results linked chemoarchitectural similarity to the physical and functional interconnectedness of brain regions (*Hansen et al., 2022*).

We first aimed to compare gradients between these architectural modalities and focused on the first two gradients of SC and FC, and the first gradient of MPC due to the respective amounts of variances explained. RC G1 showed strongest overlaps to SC G1 and FC G1 as these gradients shared either anterior-posterior or visual-to-somatomotor trajectories (*Figure 4A*). Additional weaker correlations were observed with BB G1 and MPC G1, which represent the main axes of cortical cytoarchitectural similarity (*Paquola et al., 2019*),

and FC G2, which separates unimodal from association cortices (*Margulies et al., 2016*). Functional network decoding revealed that RC G1 separates visuo- limbic from somatomotor cortices (*Figure 4—figure supplement 1*). Similar to the first receptome gradient, RC G2 correlated significantly to SC G1 and FC G1, while separating visuo- limbic from control networks (*Figure 4—figure supplement 1*). RC G3 showed the strongest correlations to SC G2, which separated occipital from temporal cortex. Further significant correlations existed with FC G1, MPC G1, and BB G1. Functional network decoding placed visual and limbic networks on opposite ends of RC G3 (*Figure 4—figure supplement 1*).

After comparing main anatomical axes, we investigated node-level similarities between the receptome and FC, SC and MPC. We performed row-wise correlations of the receptome matrix to each other matrix (*Figure 4B*). The resulting correlation coefficients expressed the strength of coupling between two measures. Generally, coupling strength of the receptome to the other measures decreased along a sensory- fugal gradient of laminar differentiation, an influential theoretical framework that attributes cognitive processing complexity to cortical areas using cytoarchitectural classes (*Mesulam, 1998*). Average coupling strength across cytoarchitectural classes was significantly different across all metrics. RC- SC decoupling along the sensory- fugal gradient (Kruskal–Wallis'  $h = 24.43$ ,  $p < 0.001$ ) was driven by significantly stronger coupling in idiosyncratic relative to heteromodal and paralimbic cortices (post hoc Dunn's test with Bonferroni correction  $p < 0.001$ ). RC- FC coupling strengths in idiosyncratic cortices were significantly increased relative to unimodal, heteromodal, and paralimbic cortices ( $h = 16.68$ ,  $p < 0.001$ ; Dunn's test  $p < 0.02$ ). Last, RC- MPC decoupling across cytoarchitectural classes ( $h = 9.16$ ,  $p < 0.05$ ) was primarily reflected by decreased coupling in heteromodal versus idiosyncratic regions (Dunn's test  $p < 0.02$ ).

As previous decoding results hinted at a relationship between cortical hierarchy and chemoarchitectural characteristics, we last explored cortical receptomic heterogeneity in the context of cytoarchitectural classes (*Mesulam, 1998*). To this end, we leveraged the Leiden community detection algorithm to discover cortical communities of chemoarchitectural similarity. We observed that new communities primarily formed in the frontal cortex when sampling the resolution parameter space, indicating more unique NTRM fingerprints in the frontal cortex. To capture how stably receptomic communities recapitulate cytoarchitectural classes when increasing the number of receptomic communities detected, we developed the

modular stability score (see ‘Materials and methods’). A cytoarchitectural class largely covered by a single receptomic community and not increasingly fracturing with an increase in the overall number of communities has a high modular stability score. Overall, paralimbic cortices exhibited modular stability similar to idiosyncratic cortices, while heteromodal and unimodal regions were less stable (*Figure 4D*), suggesting that idiosyncratic and paralimbic cortices contain a more homogeneous receptomic profile, while heteromodal and unimodal cortices have a more diverse chemoarchitectural landscape. We made similar observations studying the relationship of receptomic communities to networks of resting-state functional connectivity (*Thomas Yeo et al., 2011; Figure 4—figure supplement 1*).

### **Robustness analysis**

Owing to the spatial resolution of PET NTRM imaging, we chose to present our main findings in the coarse resolution of 100 Schaefer parcels. To assess validity, we replicated our analyses in Schaefer parcellations 200–400 (*Schaefer et al., 2018*). Selecting a finer granularity than 400 parcels was not reasonable due to the limited resolution of PET images (*Moses, 2011*). Receptome gradients showed good replicability across parcellations (*Figure 1—figure supplement 2*), although an increase in parcellation granularity shifted one extreme in RC G1 and RC G2 toward the temporal poles. Notably, for granularities of 200 and 400 parcels, there is a component ranking switch meaning that the pattern captured by RC G1 in the main results is captured by RC G2 in the replication, and vice versa. As gradients of rsFC, SC, and MPC also change as a function of parcellation granularity, we repeated the correlation analyses across different parcellations. The shift toward the temporal pole in RC G1 and G2 led to a clearer separation between one receptome gradient that strongly correlated to SC G1, and another one that significantly correlated to FC G2 in parcellation granularities 200 and 300 (Tables S2A–D). We additionally replicated agglomerative hierarchical clustering using different linkage methods (*Figure 2—figure supplement 2, Figure 4—figure supplement 2*).

### **Discussion**

In the present work, we investigated the chemoarchitectural anatomy of the human cerebral cortex and subcortex through quantification of interregional chemoarchitectural similarity, leveraging PET imaging-derived neurotransmitter transporter and receptor density maps of 19 different molecules. Furthermore, we

aimed to associate chemoarchitecture with imaging- derived markers of brain function and dysfunction, as well as other neuroanatomical modes. In sum, we introduce and thoroughly characterize chemoarchitectural similarity as an additional layer of macro-scale brain organization and present novel structure–function associations in the human brain.

A cornerstone technique of our study was the use of a nonlinear dimensionality reduction technique to derive gradients of the receptome, a matrix of interregional chemoarchitectural similarity. For the cortex, we characterized three receptome gradients, which together explain 42% of relative variance in cortical chemoarchitectural similarity, allowing for an insight into the main anatomical axes that account for nearly half of the cortical receptome’s differentiation. The first receptome gradient, RC G1, described an axis stretching between somato- motor regions, where it aligned significantly with the functional somato- motor network, and inferior temporal and occipital lobe. RC G1 combined key features of structural and functional organization, and established similar relationships between cortices as the organization of structural connections, captured by SC G1, which is likely driven by the distance-dependent nature of cortical wiring (*Markov et al., 2013*). It also captured meaningful variations in cytoarchitecture and functional organization, although these correlations were inconsistent across parcellation granularities. Anchoring cortices of RC G1 on the one end were involved in somato- motor and control functions, and facial recognition and abstraction functions on the other end, as revealed by topic-based functional activation decoding. Finally, RC G1 correlated significantly with cortical thickness alterations patterns associated with OCD. Taken together, the first receptome gradient captures the differences in chemoarchitectural composition between the somatomotor regions and the remaining cortex, with the most pronounced divergence outlined against visual and limbic cortices. This chemoarchitectural divide is most apparent in the NTRM distribution patterns of 5-HTT, 5-HT4, 5-HT2a, GABA<sub>A</sub> and M1 on the one side, which show high density in the temporal and occipital cortices, and NAT,  $\alpha 4\beta 2$ , H3 and VACHT on the other site, which have high pericentral and in the frontal densities. RC G1 furthermore connects NTRM density profiles to morphological changes in OCD, where the relationship to serotonin signaling is particularly interesting. Selective serotonin reuptake inhibitors (SSRIs) target 5-HTT and are the preferred pharmacological intervention to treat OCD (*Soomro et al., 2008; Lissemore et al., 2018*). Genetically, 5-HT2a and 5-HTT variants have been identified as risk factors for the development of OCD (*Taylor,*

2013), and OCD patients showed aberrant peripheral 5-HTT and 5-HT2a functionality (Delorme et al., 2005). In addition, there is emerging evidence that GABA signaling abnormalities are related to the development of OCD (Pauls et al., 2014), although conclusive evidence is lacking.

The second receptome gradient, RC G2, spanned between temporo-occipital and frontal anchors, separating the chemoarchitectural composition of visual and limbic networks from attention and control networks. This gradient separated 5-HTT, DAT, NMDA, D1, and GABA<sub>A</sub> from MU, H3, CB1, 5-HT1b, and  $\alpha 4\beta 2$ . It correlated significantly to FC G1 and SC G1. Topic-based functional activation decoding revealed that RC G2 spanned between regions linked to abstraction as well as facial and emotion recognition on the one end and regions involved in control and memory on the other end. Moreover, it associated cortical morphological alterations in BPD with features of NTRM fingerprints, where 5-HTT, DAT, and NMDA co-expression is of note. These NTRM have been implicated in genesis and treatment of BPD (Ghasemi et al., 2014; Ashok et al., 2017; Pinsonneault et al., 2011; Rao et al., 2019). Lastly, the third receptome gradient, RC G3, was anchored between occipital and temporal cortices. It separated GABA<sub>A</sub> density distribution patterns from D2, 5-HT1a, CB1, MU, 5-HT4, and VACHT. It correlated significantly to SC G2, FC G1, and gradients of cytoarchitectural differentiation. Functional topic-based decoding revealed that it separated regions involved in auditory and language processing from regions involved in attention, memory, and mental imagery. The separation of visual from limbic cortices distinguished RC G3 from the other two receptome gradients, where limbic and visual cortices were closely aligned.

As both RC G1 and RC G2 outline meaningful relationships between NTRM density profiles and disease morphology, chemoarchitectural similarity could provide novel perspectives in the understanding of the neurobiological basis underlying psychiatric diseases. Investigating NTRM fingerprints rather than focusing on single molecules could shed light on the enigmatic mechanism of actions of psychotropic drugs, especially when taking into account that most take effect through binding multiple types and classes of receptor molecules (Sullivan et al., 2015; Moraczewski and Aedma, 2022; Thase, 2008). However, our results also replicate associations between OCD and BPD and 5-HTT density patterns uncovered using different methodology on the same dataset, further indicating a relevance of this singular molecule in these diseases (Hansen et al., 2022). Moreover, both RC G1 and RC G2 capture variations in

chemoarchitectural similarity between unimodal and transmodal regions. A separation of sensory from association cortices using their architectural features is possible in multiple modes of architecture (*Paquola et al., 2019; Margulies et al., 2016*). The relevance of receptor fingerprints in differentiating sensory from association areas is in line with recent work that employed component analysis to autoradiography-derived receptor densities (*Goulas et al., 2021*). This correspondence across methodological approaches is important as PET imaging is of considerably lower resolution and cannot pick up on cortical layering as an important determinant of NTRM density (*Zilles and Amunts, 2009*). Gradient-based analysis indicated that visual and limbic cortices are relevant anchors in cortical chemoarchitectural similarity axes as they are polar at either one (RC G1 and G2) or both anchors of a gradient (RC G3). Hierarchical clustering of average NTRM densities separated both the visual and limbic network from other functional networks, mirroring clustering results obtained via autoradiography (*Zilles and Palomero-Gallagher, 2017*), and indicating more homogeneous chemoarchitectural compositions in these regions that, importantly, show little overlap between them. Summarizing the interrelationships of receptome gradients and brain structure and function, our results suggest that receptor similarity is organized in a fashion that combines organizational principles of cytoarchitectural, structural, and functional differentiation, although interrelationships to structural and functional connectivity and cytoarchitectural variation present themselves differently across parcellation granularities. Incorporating receptor similarity as a novel layer in studies of structure–function relationships could be crucial to discern a governing set of rules in hierarchical brain architecture (*García-Cabezas et al., 2019*).

Analysis of architectural correspondence on the node level showed significant decoupling of SC and FC from chemoarchitectural similarity, particularly in heteromodal and paralimbic regions, whereas primary areas showed the strongest coupling. This suggests that both structure–function as well as interstructural relationships dissociate in regions conveying more abstract cognitive processes such as attention, cognitive control, and memory (*Spreng et al., 2009; Smallwood et al., 2012; Smallwood et al., 2021; Langner et al., 2018*). Previous work showed that structural and functional connectivity is more closely linked in unimodal cortices and exhibits gradual decoupling toward transmodal cortices, a phenomenon that is hypothesized to be instrumental for human flexible cognition (*Preti and Van De Ville, 2019; Liu et al., 2022; Valk et al., 2022*). Replicating this observation for chemoarchitectural similarity

suggests that diversification of NTRM fingerprints may be equally important to enable flexible cognitive functions (*Suárez et al., 2020*). We corroborate this hypothesis through clustering analysis, where functional networks involved in more abstract cognitive functions and heteromodal cortices show greater receptomic diversity, meaning a wider spread of receptor fingerprints represented in them. This is consistent with associative areas showing high segregation into subareas based on their receptor architecture (*Amunts et al., 2010*). High receptomic diversity might be a disease vulnerability factor as recent work has shown that cortical thickness alterations across different diseases are most pronounced in heteromodal cortices (*Hettwer et al., 2022*). However, it has to be noted that primary regions show a lesser degree of interindividual neuroanatomical variability compared to heteromodal regions, which could be a possible methodological confound influencing our finding of sensory- to- fugal architectural decoupling (*Mueller et al., 2013*). Notably, our results exemplify a chemoarchitectural divide between heteromodal and paralimbic cortices as the latter showed NTRM co-distribution homogeneity similar to idiosyncratic cortices. A mechanistic explanation might be that, next to memory and emotion (*RajMohan and Mohandas, 2007*), olfactory areas are also located in paralimbic cortices, adding a sensory component to their function (*Courtiol and Wilson, 2017*). Additionally, recent work has indicated a differentiation between heteromodal and paralimbic regions, where the former show decreased heritability and cross-species similarity (*Valk et al., 2022*). Further work may focus on uncovering the developmental mechanisms underlying the differentiation between structure and function of these transmodal zones, also taking into account its diverging chemoarchitecture.

Finally, we could expand a chemoarchitecturally driven structure–function relationship observed in the cortex (*Morosan et al., 2005; Dehaene et al., 2005; Zilles et al., 2015; Zilles and Palomero-Gallagher, 2017*) to subcortical nuclei. Hierarchical agglomerative clustering of NTRM fingerprints revealed a meaningful separation of subcortical structures based on their functionality, exemplified by the differentiation of striatal structures (putamen, accumbens, and caudate nuclei) and pallidal globe from thalamus. Striatum and pallidal globe constitute the basal ganglia, which, together with the thalamus, form the cortico-basal ganglia-thalamic loop. Here, basal ganglia are implicated in motor functions and complex signal integration, while the thalamus orchestrates the communication between large-scale cortical networks (*Bell and Shine, 2016; Hwang et al., 2017; Lanciego et al., 2012*). This functional divide is not only reflected in NTRM fingerprints, but also in receptomic Leiden

clustering and gradient decomposition, where the first subcortical receptomic gradient describes a striato- thalamic axis. We observed partial similarity in NTRM fingerprint composition driving subcortical and cortical chemoarchitectural similarity. While differences in co-d istribution patterns of 5- HT4 and M1 from  $\alpha 4\beta 2$  and NAT were relevant in both cortex and subcortex, the two areas differ in other relevant NTRM co-d istribution patterns. For example, 5-HTT and  $\alpha 4\beta 2$  distributions in the cortex are prominently anticorrelated but show similar distributions in subcortical nuclei. Irrespective of individual NTRM co- expressions, a general similarity in subcortical and cortical receptome organization is indicated by overlapping cortical and subcortico-c ortical receptome gradients. Considering similarities and differences in NTRM fingerprints could be important when investigating the modulating influence of subcortico- cortical projections on functional brain networks (*Bell and Shine, 2016; Janacsek et al., 2022*).

### **Limitations**

It is of note that the resource we used to comprise the receptome, while extensive, does not exhaustively cover all cerebral neurotransmitter systems. Important molecules such as the  $\alpha 2$  noradrenaline receptor, which is an important drug target in the central nervous system (*Smith and Elliott, 2001; Alam et al., 2013*), are missing from our dataset. Our findings must be viewed with the incompleteness of our primary resource in mind. Additionally, we want to point out that in assessing chemoarchitectural anatomy we decided to study ionotropic receptors, metabotropic receptors, and transporters within a shared framework as they exert influence over each other in complex synaptic signaling processes. For example, D1 and D2 signaling influence NMDA signaling through cAMP-m ediated posttranslational modification of the receptor, directly acting upon its neuromodulatory potential (*Neve et al., 2004*). Similarly, neuromodulation through presynaptic transporters is conjunct with receptor expression. For example, the neuromodulatory potency of 5-H TT depends on the postsynaptic availability of serotonin receptors, which would mediate the effect an inhibition of these molecules via a drug, such as Fluoxetine. We therefore argue that when studying the co- expression of molecules involved in neurotransmission, incorporating different receptor types and transporters is crucial, even though these molecules convey different functionalities and are not interchangeable. Regarding our primary resource, while PET scans were performed on healthy participants, information on medication and medical history was not available for all participants. Therefore, we cannot control for potential

medication or disease effects. Additionally, the comparatively low spatial resolution of PET imaging is exacerbated by the group-average nature of our dataset. This especially limits the ability to investigate subcortical structures. For example, the thalamus consists of more than 60 nuclei with distinct cellular composition and diverging functionality (*Fama and Sullivan, 2015*), important properties we cannot pick up on. Other important subcortical structures, for example, the subthalamic nuclei, cannot be confidently studied due to their size, limiting our whole-brain perspective to larger subcortical nuclei. A more detailed analysis of the subcortical receptome will require methods with higher resolution (*Gaudin et al., 2019*). Furthermore, we want to point out that, although we employ structural and functional measures to contextualize our findings about chemoarchitectural anatomy, our results do not allow claims about the influence of these anatomical axes of brain function, or their interaction with structural brain elements. The correlative nature of our results enables both a richer and multifaceted characterization of chemoarchitectural anatomy as well as the formulation of hypotheses about the role of chemoarchitecture in functional specialization, but no causal inferences about how chemoarchitecture influences brain structure and function can be derived from them. Dissecting how manipulations in the chemoarchitectural landscape influence structure and function goes beyond the descriptive scope of the current work.

In sum, our work outlines the organization of chemoarchitectural similarity across the cortex and subcortical structures, yielding an additional layer of brain organization associated with structural and functional measures of brain organization in both health and disease. Considering this layer in future studies could prove important in answering how flexible cognition is supported by its physical substrates. Meeting this ultimate goal will provide new avenues to understand, treat, and prevent psychiatric diseases and lessen both the personal and societal burden posed by mental illnesses.

## **Materials and methods**

### **Receptor similarity matrix generation**

To investigate cortical and subcortical receptor similarity, we made use of an open-access PET MRI dataset described previously (*Hansen et al., 2022*). The associated receptors/transporters, tracers, number of healthy participants, ages, and original publications, for which we refer to full methodological details, are listed in Table S1.

In brief, images were acquired in healthy participants using best practice imaging protocols recommended for each radioligand (*Nørgaard et al., 2019*) and averaged across participants before being shared. Images were registered to the MNI152 template (2009c, asymmetric). No medication history of participants was available. The accuracy and validity of receptor density as derived from the PET images have been confirmed using autoradiography data, and the mean age of participants was shown to have negligible influence on tracer density values (*Hansen et al., 2022*). The cortical receptor density maps were parcellated to 100, 200, 300, and 400 regions based on the Schaefer parcellation (*Schaefer et al., 2018*), averaging the intensity values per parcel. Subcortical NTRM densities were extracted using a functional connectivity-derived topographic atlas (*Tian et al., 2020*). For tracers where more than one study was included, a weighted average was generated. This resulted in a parcel  $\times$  19 matrix of format (parcel  $\times$  receptor). The intensity values were z-score normalized per tracer. We then performed parcel  $\times$  parcel Spearman rank correlation of receptor densities, yielding the receptome, a matrix of interregional NTRM similarity.

### **Gradient decomposition**

To assess the driving axes of cortical and subcortical architectural covariance organization, we employed gradient decomposition using the brainspace python package (*Vos de Wael et al., 2020*). Gradients are low-d imensional manifold representations that allow for the characterization of main organizational principles of high-dimensional data (*Margulies et al., 2016*). To calculate gradients of cortical NTRM covariance, rsFC, and MPC, the full matrix was used. SC gradients were separately calculated for intrahemispheric connections in both hemispheres using procrustes analysis to align the gradients to increase comparability and subsequently concatenated. We excluded interhemispheric connections due to their biased underdetection in dMRI fiber tracking, which would result in gradient decomposition primarily detecting asymmetric interhemispheric axes that are unlikely to possess neurobiological relevance, but rather reflect the aforementioned bias (*Royer et al., 2022*). To calculate the gradients, the respective input matrices were thresholded at 90% and, using a normalized angle similarity kernel, transformed into a square non-negative affinity matrix. We then applied diffusion embedding (*Coifman and Lafon, 2006*), a nonlinear dimensionality reduction technique, to extract a low-d imensional embedding of the affinity matrix. Diffusion embedding projects network nodes into a common gradient space, where their distance is a function of connection strengths. This means that nodes closely

together in this space display either many suprathreshold or few very strong connections, while nodes distant in gradient space display weak to no connections. In diffusion embedding, a parameter  $\alpha$  controls the influence of sampling density on the underlying manifold (where  $\alpha = 0$  equals no influence and  $\alpha = 1$  equals maximal influence). Similar to previous work (*Margulies et al., 2016*), we set  $\alpha$  to 0.5 to retain global relations in the embedded space and provide robustness to noise in the original matrix.

### **Structural, functional, and microstructural profile covariance data generation**

To contextualize receptor similarity organization, we aimed to compare it to SC, resting- state FC, and MPC. The diversity pertaining to age and sociodemographic variables of the subjects in the PET dataset made the selection of matched reference subjects for FC, SC, and MPC analysis infeasible. Instead, we opted for the construction of group- consensus FC, SC, and MPC matrices collected from the same healthy individuals, obtained, and processed in a reproducible pipeline to ultimately provide comparability of the receptome to SC, FC, and MPC measures of reference nature. We therefore chose the Microstructure Informed Connectomics (MICA-M ICs) dataset (*Royer et al., 2022*) to obtain FC, SC, and MPC data. MRI data was acquired at the Brain Imaging Centre of the Montreal Neurological Institute and Hospital using a 3T Siemens Magnetom Prisma-F it equipped with a 64- channel head coil from 50 healthy young adults with no prior history of neurological or mental illnesses (23 women;  $29.54 \pm 5.62$  y). No medication history was available. For each participant, (1) a T1-w eighted (T1w) structural scan, (2) multi- shell diffusion-w eighted imaging (DWI), (3) resting- state functional MRI (rs- fMRI), and (4) a second T1-w eighted scan, followed by quantitative T1 (qT1) mapping. Image preprocessing was performed via micapipe, an open- access processing pipeline for multimodal MRI data (*Cruces et al., 2022*). Individual functional connectomes were generated by averaging rs- fMRI time series within cortical parcels and cross- correlating all nodal time series. Individual structural connectomes were defined as the weighted count of tractography- derived whole- brain streamlines. To estimate individual microstructural profile covariance, 14 equivolumetric surfaces were generated to sample vertex- wise qT1 intensities across cortical depths and subsequently averaged within parcels. Parcel- level qT1 intensity values were cross- correlated using partial correlations while controlling for the average cortical intensity profile. The resulting values were log- transformed to obtain the individual MPC matrices (*Paquola et al., 2019*).

To generate the group-average matrix of each modality, precomputed and pre-parcellated matrices of 50 individual subjects were used. As no PET data was available for the medial wall, the rows and columns representing it in all SC, FC, and MPC matrices were discarded. For SC and FC matrices additionally, rows and columns containing values for subcortical regions were discarded as well as no analysis of subcortical SC and FC was intended. To generate the group-consensus MPC matrix, parcel values across the subjects were averaged. To generate the group-consensus FC matrix, the subject matrices underwent Fisher's  $r$ -to- $z$  transformation, and subsequently, parcel values across the subjects were averaged. To generate the group-consensus SC matrix, individual matrices were log-transformed and parcel values across subjects were averaged. Afterward, we applied distance-dependent thresholding to account for the over-representation of short-range and under-representation of long-range connections in non-thresholded group-consensus SC matrices (*Betzel et al., 2019*), and the resulting thresholded matrix was used in subsequent analyses.

### **Coupling analysis**

To investigate the coupling between receptor similarity and FC, SC, and MPC, we performed row-wise Spearman rank correlation analyses of the nonzero elements of the respective matrices.

### **Leiden clustering**

To evaluate whether NTRM similarity intrinsically structures the cortical surface and subcortical structures, we applied the Leiden clustering algorithm (*Traag et al., 2019*). This clustering analysis enables an assessment of how similarity in chemoarchitecture forms anatomical communities, akin to approaches used to reveal resting-state functional networks (*Thomas Yeo et al., 2011*) or parcellations (*Schaefer et al., 2018*). The Leiden algorithm is a greedy optimization method that aims to maximize the number of within-group edges and minimize the number of between-group edges, with the resulting network modularity being governed by the resolution parameter  $\gamma$ . To incorporate anticorrelations, we used a negative-asymmetric approach, meaning that we aimed to maximize positive edge weights within communities and negative edge weights between communities. To search the feature space, we chose a  $\gamma$  range of 0.5–10 in increments of 0.05 for cortical data, calculating 1000 partition solutions per  $\gamma$ . For subcortical structures, we chose a  $\gamma$  range of 1–10 in increments of 0.5, calculating 250 partitions per  $\gamma$ . To assess partition stability, we calculated the  $z$ -score for every partition with every other partition per  $\gamma$  value and chose the

partition with the highest mean z-r and score, indicating highest similarity to all other partitions for the given  $\gamma$  (Steinley, 2004; Pedregosa et al., 2023). Additionally, we calculated the variance of z-rand scores between partitions per  $\gamma$ . A high mean z-rand score and a low z-rand score variance indicated a stable partition solution.

### **Modular stability**

To assess the overlap of cytoarchitectural classes and receptive clustering, we developed the modular stability score. This metric captures how far a predefined ROI, in our case, a functional network or a cytoarchitectural class, matches a Leiden clustering-derived receptive community. It is calculated as  $C_{max} \times (C_{in} + 1) / C_{tot} \times s$ , where  $C_{max}$  is the biggest proportion of the ROI is taken up by one clustering-derived receptive community,  $C_{in}$  is the number of different receptive communities represented inside the ROI,  $C_{tot}$  is the total number of receptive communities formed at the given resolution parameter, and  $s$  is the relative size of the ROI. An ROI that is covered by one receptive community to a large degree and does not contain a relatively large number of receptive communities, as measured by the proportion of communities inside the region of interest divided by the total number of communities, will display a high modular stability score. As larger ROIs will have a higher number of communities inside them by chance, we normalize by the relative size of the ROI. We then employ the modular stability score to quantify to what degree predefined ROIs break up into different receptive communities as the clustering-derived network modularity increases as we sample the resolution parameter space. Note that this experimental score has not been used and verified for validity under other conditions.

### **Meta-analytic decoding**

To assess the relationship between cortical receptive gradients and localized brain functionality, we leveraged meta-analytical, topic-based maps of functional brain activation, derived from the Neurosynth database (Tor D., 2011). Using Nimare, we calculated topic-based activation maps of the Neurosynth v5-50 topic release (<https://neurosynth.org/analyses/topics/v5-topics-50/>), a set of 50 topics extracted from the abstracts in the full Neurosynth database as of July 2018 using Latent Dirichlet Analysis (Poldrack et al., 2012). We parcellated the resulting continuous, non-thresholded activation maps and performed parcel-wise Spearman rank correlations with the cortical receptive gradients.

## Disorder impact

To assess the relationship between receptome gradients and various neurological and psychiatric diseases, we used publicly available multisite summary statistics of cortical thinning published by the ENIGMA Consortium (*Thompson et al., 2014*). Covariate-adjusted case- vs.-control differences, denoted by across-site random-effects meta-analyses of Cohen's  $d$ -values for cortical thickness, were acquired through the ENIGMA toolbox python package (*Larivière et al., 2021*). Multiple linear regression analyses were used to fit age, sex, and site information to cortical thickness measures. Before computing summary statistics, raw data was preprocessed, segmented, and parcellated according to the Desikan-Killiany atlas in FreeSurfer (<http://surfer.nmr.mgh.harvard.edu>) at each site and according to standard ENIGMA quality control protocols (see <http://enigma.ini.usc.edu/protocols/imaging-protocols>). To assess a diverse range of cerebral illnesses, we included eight diseases in our analysis: ASD (*van Rooij et al., 2018*), ADHD (*Hoogman et al., 2019*), BPD (*Hibar et al., 2018*), DiGeorge-syndrome (22q11.2 deletion syndrome) (DGS) (*Sun et al., 2020*), EPS (*Whelan et al., 2018*), MDD (*Schmaal et al., 2017*), OCD (*Boedhoe et al., 2018*), and SCZ (*van Erp et al., 2018*). Sample sizes ranged from 1272 (ADHD) to 9572 (SCZ). Summary statistics were derived from adult samples, except for ASD, where all age ranges were used.

## Hierarchical clustering

To discern a similarity hierarchy of subcortical structures and cortical networks based on mean NTRM density, we performed agglomerative hierarchical clustering. Initially, a set of  $n$  samples consists of  $m$  clusters, where  $m = n$ . In an iterative approach, the samples that are most similar are combined into a cluster, where after each iteration, there are  $m - \#$  iteration clusters (*Nielsen, 2016*). This process is repeated until  $m = 1$ . We use Euclidean distance to assess the distance between clusters and use the WPGMA method to select the closest pair of subsets (*Sokal et al., 1958*).

## Null models

Assessment of statistical significance in brain imaging data may be biased when not accounting for spatial autocorrelation of brain imaging signals (*Alexander-Bloch et al., 2018; Váša and Mišić, 2022*). To generate permuted brain maps that preserve spatial autocorrelation in parcellated data, we resorted to variogram matching (VGM) (*Burt et al., 2020*). Here, we randomly shuffle the input data and then apply distance-dependent smoothing and rescaling to recover spatial autocorrelation. To assess the

significance when comparing surface-projected data, we applied spin permutation (*Alexander-Bloch et al., 2018*) to generate randomly permuted brain maps by random-angle spherical rotation of surface-projected data points, which preserves spatial autocorrelation. Parcel values that got rotated into the medial wall, and values from the medial wall that got rotated to the cortical surface, were discarded (*Markello and Misic, 2021*). In each approach, we generated 1000 permuted brain maps.

## Acknowledgements

We thank Nicola Palomero-Gallagher and Thomas Funck for helpful discussions. We acknowledge and thank those who openly shared their data with the neuroscientific community, which enabled us to perform our study, including the PIs involved in the PET scanning, the MICA-MICS dataset, the Neurosynth tool, as well as all members of the ENIGMA consortium working groups.

## Additional information

### Funding

Funder	Grant reference number	Author
Max-Planck-Institut Kognitions- und Neurowissenschaften	Open Access funding für	Sofie Louise Valk
Helmholtz International BigBrain Analytics & Laboratory		Justine Y Hansen Boris C Bernhardt Simon B Eickhoff Sofie Louise Valk
Natural Sciences and Engineering Research Council of Canada		Justine Y Hansen Boris C Bernhardt Bratislav Misic
Canadian Institutes of Health Research		Boris C Bernhardt Bratislav Misic
Brain Canada Foundation Future Leaders Fund		Boris C Bernhardt Bratislav Misic
Canada Research Chairs		Bratislav Misic
Michael J. Fox Foundation for Parkinson's Research		Bratislav Misic
Sick Kids Foundation	NI17-039	Boris C Bernhardt
Azrieli Center for Autism Research	ACAR-TACC	Boris C Bernhardt
Fonds de Recherche du Québec - Santé		Boris C Bernhardt

Tier-2 Canada Research Chairs program		Boris C Bernhardt
Human Brain Project		Simon B Eickhoff
Helmholtz International Lab grant agreement	InterLabs-0015	Boris C Bernhardt Simon B Eickhoff Sofie Louise Valk
Canada First Research Excellence Fund	CFREF Competition 2	Boris C Bernhardt Simon B Eickhoff Sofie Louise Valk
Horizon 2020	No. 826421 "TheVirtualBrain-Cloud"	Juergen Dukart
Canada First Research Excellence Fund	2015-2016	Boris C Bernhardt
Max Planck Society	Otto Hahn Award	Sofie Louise Valk

Open access funding provided by Max Planck Society. The funders had no role in study design, data collection and interpretation, or the decision to submit the work for publication.

#### Author contributions

Benjamin Hänisch, Conceptualization, Data curation, Investigation, Visualization, Methodology, Writing - original draft, Writing - review and editing; Justine Y Hansen, Data curation, Investigation, Writing - review and editing; Boris C Bernhardt, Software, Methodology, Writing - review and editing; Simon B Eickhoff, Supervision, Writing - review and editing; Juergen Dukart, Bratislav Mistic, Data curation, Writing - review and editing; Sofie Louise Valk, Conceptualization, Supervision, Investigation, Visualization, Methodology, Writing - original draft, Writing - review and editing

#### Author ORCIDs

Benjamin Hänisch   
<http://orcid.org/0000-0001-5463-4218>

Justine Y Hansen  
<http://orcid.org/0000-0003-3142-7480>

Boris C Bernhardt  
<http://orcid.org/0000-0001-9256-6041>

Simon B Eickhoff  
<http://orcid.org/0000-0001-6363-2759>

Juergen Dukart   
<http://orcid.org/0000-0003-0492-5644> Bratislav Mistic   
<http://orcid.org/0000-0003-0307-2862>

Sofie Louise Valk   
<http://orcid.org/0000-0003-2998-6849>

#### Ethics

Human subjects: The current research complies with all relevant ethical regulations as set by The Independent Research Ethics Committee at the Medical Faculty of the Heinrich- Heine- University of Duesseldorf (study number 2018- 317). The current data was based on open access resources, and ethic approvals of the individual datasets are available in the original publications of each data source.

#### Decision letter and Author response

Decision letter <https://doi.org/10.7554/eLife.83843.sa1>

Author response <https://doi.org/10.7554/eLife.83843.sa2>

---

## Additional files

### Supplementary files

- Supplementary file 1. Table S1. Neurotransmitter receptors and transporters included in analyses. BPND, non- displaceable binding potential; VT, tracer distribution volume; Bmax, density (pmol/ml) converted from binding potential or distributional volume using autoradiography- derived densities; SUVR, standard uptake value ratio. Neurotransmitter receptor maps without citations refer to unpublished data. Table adapted from *Hansen et al., 2022*.
- Supplementary file 2. Table S2A. Replication of multimodal receptome gradient contextualization through correlation using a Schaefer granularity of 100 parcels.
- Supplementary file 3. Table S2B. Replication of multimodal receptome gradient contextualization through correlation using a Schaefer granularity of 200 parcels.
- Supplementary file 4. Table S2C. Replication of multimodal receptome gradient contextualization through correlation using a Schaefer granularity of 300 parcels.
- Supplementary file 5. Table S2D. Replication of multimodal receptome gradient contextualization through correlation using a Schaefer granularity of 400 parcels.

- MDAR checklist

#### Data availability

All data and software used in this study is openly accessible. PET data is available [here](#). FC, SC and MPC data is available [here](#). ENIGMA data is available through [enigmatoolbox](#). Meta-analytical functional activation data is available through [Neurosynth](#). The code used to perform the analyses can be found [here](#).

The following previously published datasets were used:

Author(s)	Year	Dataset title	Dataset URL	Database and Identifier
Hansen JY, Shafiei G, 2022 Markello RD, Smart K, Cox SML, Nørgaard M		Mapping neurotransmitter systems to the structural receptors of the human neocortex	<a href="https://github.com/netneurolab/hansen_and_functional_organization">https://github.com/netneurolab/hansen_and_functional_organization</a>	GitHub, hansen_receptor_and_functional_organization

*Continued on next page*

*Continued*

Author(s)	Year	Dataset title	Dataset URL	Database and Identifier
Royer J, Rodríguez-Cruces R, Tavakoli S, Larivière S, Herholz P, Li Q, Vos de Wael R, Paquola C, Benkarim O, Park BY, Lowe AJ, Margulies D, Smallwood J, Bernasconi A, Bernasconi N, Frauscher B, Bernhardt BC	2021	MICA- MICs: a dataset for Microstructure- Informed Connectomics	<a href="https://n2t.net/ark:/70798/d72xnk2wd397j190qv">https://n2t.net/ark:/70798/d72xnk2wd397j190qv</a>	Canadian Open Neuroscience Platform, 70798/d72xnk2wd397j190qv

## References

Alam A, Voronovich Z, Carley JA. 2013. A review of therapeutic uses of mirtazapine in psychiatric and medical conditions. *The Primary Care Companion for CNS Disorders* **15**:PCC.13r01525. DOI: <https://doi.org/10.4088/PCC.13r01525>, PMID: 24511451

Alexander- Bloch AF, Shou H, Liu S, Satterthwaite TD, Glahn DC, Shinohara RT, Vandekar SN, Raznahan A. 2018.

On testing for spatial correspondence between maps of human brain structure and function. *NeuroImage* **178**:540–551. DOI: <https://doi.org/10.1016/j.neuroimage.2018.05.070>

Amunts K, Lenzen M, Friederici AD, Schleicher A, Morosan P, Palomero- Gallagher N, Zilles K. 2010. Broca's region: novel organizational principles and multiple receptor mapping. *PLOS Biology* **8**:e1000489. DOI: <https://doi.org/10.1371/journal.pbio.1000489>, PMID: 20877713

Amunts K, Lepage C, Borgeat L, Mohlberg H, Dickscheid T, Rousseau MÉ, Bludau S, Bazin PL, Lewis LB, Oros- Peusquens AM, Shah NJ, Lippert T, Zilles K, Evans AC. 2013. BigBrain: An ultrahigh- resolution 3D human brain model. *Science* **340**:1472–1475. DOI: <https://doi.org/10.1126/science.1235381>, PMID: 23788795

Ashok AH, Marques TR, Jauhar S, Nour MM, Goodwin GM, Young AH, Howes OD. 2017. The dopamine hypothesis of bipolar affective disorder: The state of the art and implications for treatment. *Molecular Psychiatry* **22**:666–679. DOI: <https://doi.org/10.1038/mp.2017.16>

- Bell PT, Shine JM. 2016. Subcortical contributions to large- scale network communication. *Neuroscience and Biobehavioral Reviews* **71**:313–322. DOI: <https://doi.org/10.1016/j.neubiorev.2016.08.036>, PMID: 27590830
- Betzel RF, Griffa A, Hagmann P, Mišić B. 2019. Distance- dependent consensus thresholds for generating group- representative structural brain networks. *Network Neuroscience* **3**:475–496. DOI: [https://doi.org/10.1162/netn\\_a\\_00075](https://doi.org/10.1162/netn_a_00075), PMID: 30984903
- Boedhoe PSW, Schmaal L, Abe Y, Alonso P, Ameis SH, Anticevic A, Arnold PD, Batistuzzo MC, Benedetti F, Beucke JC, Bollettini I, Bose A, Brem S, Calvo A, Calvo R, Cheng Y, Cho KIK, Ciullo V, Dallspezia S, Denys D, et al. 2018. Cortical abnormalities associated with pediatric and adult obsessive- compulsive disorder: Findings from the ENIGMA obsessive- compulsive disorder working group. *The American Journal of Psychiatry* **175**:453–462. DOI: <https://doi.org/10.1176/appi.ajp.2017.17050485>, PMID: 29377733
- Brodmann K. 1909. *Vergleichende Lokalisationslehre Der Grosshirnrinde in Ihren Prinzipien Dargestellt Auf Grund Des Zellenbaues* Barth.
- Burt JB, Helmer M, Shinn M, Anticevic A, Murray JD. 2020. Generative modeling of brain maps with spatial autocorrelation. *NeuroImage* **220**:117038. DOI: <https://doi.org/10.1016/j.neuroimage.2020.117038>, PMID: 32585343
- Cipriani A, Furukawa TA, Salanti G, Chaimani A, Atkinson LZ, Ogawa Y, Leucht S, Ruhe HG, Turner EH, Higgins JPT, Egger M, Takeshima N, Hayasaka Y, Imai H, Shinohara K, Tajika A, Ioannidis JPA, Geddes JR. 2018. Comparative efficacy and acceptability of 21 antidepressant drugs for the acute treatment of adults with major depressive disorder: A systematic review and network meta- analysis. *The Lancet* **391**:1357–1366. DOI: [https://doi.org/10.1016/S0140-6736\(17\)32802-7](https://doi.org/10.1016/S0140-6736(17)32802-7)
- Coifman RR, Lafon S. 2006. Diffusion maps. *Applied and Computational Harmonic Analysis* **21**:5–30. DOI: <https://doi.org/10.1016/j.acha.2006.04.006>
- Courtiol E, Wilson DA. 2017. The olfactory mosaic: Bringing an olfactory network together for odor perception. *Perception* **46**:320–332. DOI: <https://doi.org/10.1177/0301006616663216>, PMID: 27687814
- Cruces RR, Royer J, Herholz P, Larivière S, Vos de Wael R, Paquola C, Benkarim O, Park BY, Degré-Pelletier J, Nelson MC, DeKraker J, Leppert IR, Tardif C, Poline JB, Concha L, Bernhardt BC. 2022. Micapipe: A pipeline for multimodal neuroimaging and connectome analysis. *NeuroImage* **263**:119612. DOI: <https://doi.org/10.1016/j.neuroimage.2022.119612>, PMID: 36070839
- Dean J, Keshavan M. 2017. The neurobiology of depression: An integrated view. *Asian Journal of Psychiatry* **27**:101–111. DOI: <https://doi.org/10.1016/j.ajp.2017.01.025>
- Dehaene S, Duhamel JR, Hauser MD, Rizzolatti G. 2005. *From Monkey Brain to Human Brain: A Fyssen Foundation Symposium* MIT press. DOI: <https://doi.org/10.7551/mitpress/3136.001.0001>
- Delorme R, Betancur C, Callebort J, Chabane N, Laplanche J-L, Mouren- Simeoni M- C, Launay J- M, Leboyer M. 2005. Platelet serotonergic markers as endophenotypes for obsessive- compulsive disorder. *Neuropsychopharmacology* **30**:1539–1547. DOI: <https://doi.org/10.1038/sj.npp.1300752>, PMID: 15886722
- Dukart J, Holiga S, Rullmann M, Lanzenberger R, Hawkins PCT, Mehta MA, Hesse S, Barthel H, Sabri O, Jech R, Eickhoff SB. 2021. JuSpace: A tool for spatial correlation analyses of magnetic resonance imaging data with nuclear imaging derived neurotransmitter maps. *Human Brain Mapping* **42**:555–566. DOI: <https://doi.org/10.1002/hbm.25244>, PMID: 33079453
- Eickhoff SB, Rottschy C, Zilles K. 2007. Laminar distribution and co- distribution of neurotransmitter receptors in early human visual cortex. *Brain Structure and Function* **212**:255–267. DOI: <https://doi.org/10.1007/s00429-007-0156-y>

- Eickhoff SB, Rottschy C, Kujovic M, Palomero- Gallagher N, Zilles K. 2008. Organizational principles of human visual cortex revealed by receptor mapping. *Cerebral Cortex* **18**:2637–2645. DOI: <https://doi.org/10.1093/cercor/bhn024>, PMID: 18321873
- Fama R, Sullivan EV. 2015. Thalamic structures and associated cognitive functions: Relations with age and aging. *Neuroscience and Biobehavioral Reviews* **54**:29–37. DOI: <https://doi.org/10.1016/j.neubiorev.2015.03.008>, PMID: 25862940
- Foit NA, Yung S, Lee HM, Bernasconi A, Bernasconi N, Hong SJ. 2022. A whole- brain 3D myeloarchitectonic atlas: Mapping the Vogt- Vogt legacy to the cortical surface. *NeuroImage* **263**:119617. DOI: <https://doi.org/10.1016/j.neuroimage.2022.119617>, PMID: 36084859
- Forstmann BU, de Hollander G, van Maanen L, Alkemade A, Keuken MC. 2017. Towards a mechanistic understanding of the human subcortex. *Nature Reviews Neuroscience* **18**:57–65. DOI: <https://doi.org/10.1038/nrn.2016.163>
- García- Cabezas MÁ, Zikopoulos B, Barbas H. 2019. The Structural model: A theory linking connections, plasticity, pathology, development and evolution of the cerebral cortex. *Brain Structure & Function* **224**:985–1008. DOI: <https://doi.org/10.1007/s00429-019-01841-9>, PMID: 30739157
- Gaudin É, Toussaint M, Thibaudeau C, Paillé M, Fontaine R, Lecomte R. 2019. Performance simulation of an ultra- high resolution brain PET scanner using 1.2- mm pixel detectors. *IEEE Transactions on Radiation and Plasma Medical Sciences* **3**:334–342. DOI: <https://doi.org/10.1109/TRPMS.2018.2877511>, PMID: 31453423
- Geddes JR, Miklowitz DJ. 2013. Treatment of bipolar disorder. *The Lancet* **381**:1672–1682. DOI: [https://doi.org/10.1016/S0140-6736\(13\)60857-0](https://doi.org/10.1016/S0140-6736(13)60857-0)
- Ghasemi M, Phillips C, Trillo L, De Miguel Z, Das D, Salehi A. 2014. The role of NMDA receptors in the pathophysiology and treatment of mood disorders. *Neuroscience & Biobehavioral Reviews* **47**:336–358. DOI: <https://doi.org/10.1016/j.neubiorev.2014.08.017>
- Goulas A, Changeux JP, Wagstyl K, Amunts K, Palomero- Gallagher N, Hilgetag CC. 2021. The natural axis of transmitter receptor distribution in the human cerebral cortex. *PNAS* **118**:e2020574118. DOI: <https://doi.org/10.1073/pnas.2020574118>, PMID: 33452137
- Hansen JY, Shafiei G, Markello RD, Smart K, Cox SML, Nørgaard M, Beliveau V, Wu Y, Gallezot J- D, Aumont É, Servaes S, Scala SG, DuBois JM, Wainstein G, Bezgin G, Funck T, Schmitz TW, Spreng RN, Galovic M, Koepp MJ, et al. 2022. Mapping neurotransmitter systems to the structural and functional organization of the human neocortex. *Nature Neuroscience* **25**:1569–1581. DOI: <https://doi.org/10.1038/s41593-022-01186-3>, PMID: 36303070
- Harrison PJ, Geddes JR, Tunbridge EM. 2018. The emerging neurobiology of bipolar disorder. *Trends in Neurosciences* **41**:18–30. DOI: <https://doi.org/10.1016/j.tins.2017.10.006>
- Hettwer M, Larivière S, Park B, van den Heuvel O, Schmaal L, Andreassen O, Ching C, Hoogman M, Buitelaar J, Veltman D, Stein D, Franke B, van Erp T, Jahanshad N, Thompson P, Thomopoulos S, Bethlehem R, Bernhardt B, Eickhoff S, Valk S, et al. 2022. Coordinated cortical thickness alterations across psychiatric conditions: A transdiagnostic ENIGMA Study. *medRxiv*. DOI: <https://doi.org/10.1101/2022.02.03.22270326>
- Hibar DP, Westlye LT, Doan NT, Jahanshad N, Cheung JW, Ching CRK, Versace A, Bilderbeck AC, Uhlmann A, Mwangi B, Krämer B, Overs B, Hartberg CB, Abé C, Dima D, Grotegerd D, Sprooten E, Bøen E, Jimenez E, Howells FM, et al. 2018. Cortical abnormalities in bipolar disorder: an MRI analysis of 6503 individuals from the ENIGMA Bipolar Disorder Working Group. *Molecular Psychiatry* **23**:932–942. DOI: <https://doi.org/10.1038/mp.2017.73>, PMID: 28461699

- Hoogman M, Muetzel R, Guimaraes JP, Shumskaya E, Mennes M, Zwiers MP, Jahanshad N, Sudre G, Wolfers T, Earl EA, Soliva Vila JC, Vives- Gilabert Y, Khadka S, Novotny SE, Hartman CA, Heslenfeld DJ, Schieren LJS, Ambrosino S, Oranje B, de Zeeuw P, et al. 2019. Brain imaging of the cortex in ADHD: A coordinated analysis of large- scale clinical and population-based samples. *The American Journal of Psychiatry* **176**:531–542. DOI: <https://doi.org/10.1176/appi.ajp.2019.18091033>, PMID: 31014101
- Huhn M, Nikolakopoulou A, Schneider- Thoma J, Krause M, Samara M, Peter N, Arndt T, Bäckers L, Rothe P, Cipriani A, Davis J, Salanti G, Leucht S. 2019. Comparative efficacy and tolerability of 32 oral antipsychotics for the acute treatment of adults with multi- episode schizophrenia: A systematic review and network meta- analysis. *The Lancet* **394**:939–951. DOI: [https://doi.org/10.1016/S0140-6736\(19\)31135-3](https://doi.org/10.1016/S0140-6736(19)31135-3), PMID: 31320283
- Hwang K, Bertolero MA, Liu WB, D’Esposito M. 2017. The human thalamus is an integrative hub for functional brain networks. *The Journal of Neuroscience* **37**:5594–5607. DOI: <https://doi.org/10.1523/JNEUROSCI.0067- 17.2017>, PMID: 28450543
- Janacek K, Evans TM, Kiss M, Shah L, Blumenfeld H, Ullman MT. 2022. Subcortical cognition: The fruit below the rind. *Annual Review of Neuroscience* **45**:361–386. DOI: <https://doi.org/10.1146/annurev-neuro-110920- 013544>, PMID: 35385670
- Kaltenboeck A, Harmer C. 2018. The neuroscience of depressive disorders: A brief review of the past and some considerations about the future. *Brain and Neuroscience Advances* **2**:2398212818799269. DOI: <https://doi.org/ 10.1177/2398212818799269>, PMID: 32166149
- Kesby JP, Eyles DW, McGrath JJ, Scott JG. 2018. Dopamine, psychosis and schizophrenia: The widening gap between basic and clinical neuroscience. *Translational Psychiatry* **8**:30. DOI: <https://doi.org/10.1038/s41398- 017-0071-9>, PMID: 29382821
- Lanciego JL, Luquin N, Obeso JA. 2012. Functional neuroanatomy of the basal ganglia. *Cold Spring Harbor Perspectives in Medicine* **2**:a009621. DOI: <https://doi.org/10.1101/cshperspect.a009621>, PMID: 23071379
- Langner R, Leiberg S, Hoffstaedter F, Eickhoff SB. 2018. Towards a human self- regulation system: Common and distinct neural signatures of emotional and behavioural control. *Neuroscience and Biobehavioral Reviews* **90**:400–410. DOI: <https://doi.org/10.1016/j.neubiorev.2018.04.022>, PMID: 29730485
- Larivière S, Paquola C, Park B- Y, Royer J, Wang Y, Benkarim O, Vos de Wael R, Valk SL, Thomopoulos SI, Kirschner M, Lewis LB, Evans AC, Sisodiya SM, McDonald CR, Thompson PM, Bernhardt BC. 2021. The ENIGMA Toolbox: Multiscale neural contextualization of multisite neuroimaging datasets. *Nature Methods* **18**:698–700. DOI: <https://doi.org/10.1038/s41592-021-01186-4>, PMID: 34194050
- Lissemore JI, Sookman D, Gravel P, Berney A, Barsoum A, Diksik M, Nordahl TE, Pinard G, Sibon I, Cottraux J, Leyton M, Benkelfat C. 2018. Brain serotonin synthesis capacity in obsessive- compulsive disorder: Effects of cognitive behavioral therapy and sertraline. *Translational Psychiatry* **8**:82. DOI: <https://doi.org/10.1038/ s41398-018-0128-4>, PMID: 29666372
- Liu ZQ, Vázquez- Rodríguez B, Spreng RN, Bernhardt BC, Betzel RF, Misisic B. 2022. Time- resolved structure- function coupling in brain networks. *Communications Biology* **5**:532. DOI: <https://doi.org/10.1038/s42003-022- 03466-x>, PMID: 35654886
- Logothetis NK. 2008. What we can do and what we cannot do with fMRI. *Nature* **453**:869–878. DOI: <https://doi.org/10.1038/nature06976>, PMID: 18548064
- Luvannyam E, Jain MS, Pormento MKL, Siddiqui H, Balagtas ARA, Emuze BO, Poprawski T. 2022. Neurobiology of Schizophrenia: A comprehensive review. *Cureus* **14**:e23959. DOI: <https://doi.org/10.7759/cureus.23959>, PMID: 35541299

- Lydiard RB. 2003. The role of GABA in anxiety disorders. *The Journal of Clinical Psychiatry* **64**:21–27 PMID: 12662130.
- Margulies DS, Ghosh SS, Goulas A, Falkiewicz M, Huntenburg JM, Langs G, Bezgin G, Eickhoff SB, Castellanos FX, Petrides M, Jefferies E, Smallwood J. 2016. Situating the default- mode network along a principal gradient of macroscale cortical organization. *PNAS* **113**:12574–12579. DOI: <https://doi.org/10.1073/pnas.1608282113>, PMID: 27791099
- Markello RD, Misisic B. 2021. Comparing spatial null models for brain maps. *NeuroImage* **236**:118052. DOI: <https://doi.org/10.1016/j.neuroimage.2021.118052>, PMID: 33857618
- Markov NT, Ercsey-Ravasz M, Van Essen DC, Knoblauch K, Toroczkai Z, Kennedy H. 2013. Cortical high- density counterstream architectures. *Science* **342**:1238406. DOI: <https://doi.org/10.1126/science.1238406>, PMID: 24179228
- Mesulam MM. 1998. From sensation to cognition. *Brain* **121**:1013–1052. DOI: <https://doi.org/10.1093/brain/121.6.1013>
- Moncrieff J, Cooper RE, Stockmann T, Amendola S, Hengartner MP, Horowitz MA. 2022. The serotonin theory of depression: A systematic umbrella review of the evidence. *Molecular Psychiatry*:e1661. DOI: <https://doi.org/10.1038/s41380-022-01661-0>, PMID: 35854107
- Moraczewski J, Aedma KK. 2022. *Tricyclic antidepressants* StatPearls Publishing.
- Morosan P, Schleicher A, Amunts K, Zilles K. 2005. Multimodal architectonic mapping of human superior temporal gyrus. *Anatomy and Embryology* **210**:401–406. DOI: <https://doi.org/10.1007/s00429-005-0029-1>, PMID: 16170539
- Moses WW. 2011. Fundamental limits of spatial resolution in PET. *Nuclear Instruments & Methods in Physics Research. Section A, Accelerators, Spectrometers, Detectors and Associated Equipment* **648**:S236–S240. DOI: <https://doi.org/10.1016/j.nima.2010.11.092>, PMID: 21804677
- Mueller S, Wang D, Fox MD, Yeo BTT, Sepulcre J, Sabuncu MR, Shafee R, Lu J, Liu H. 2013. Individual variability in functional connectivity architecture of the human brain. *Neuron* **77**:586–595. DOI: <https://doi.org/10.1016/j.neuron.2012.12.028>, PMID: 23395382
- Nautiyal KM, Hen R. 2017. Serotonin receptors in depression: From A to B. *F1000Research* **6**:123. DOI: <https://doi.org/10.12688/f1000research.9736.1>, PMID: 28232871
- Neve KA, Seamans JK, Trantham-Davidson H. 2004. Dopamine Receptor Signaling. *Journal of Receptors and Signal Transduction* **24**:165–205. DOI: <https://doi.org/10.1081/RRS-200029981>
- Nielsen F. 2016. Hierarchical clustering. Nielsen F (Ed). *Introduction to HPC with MPI for data science* Springer International Publishing. p. 195–211. DOI: <https://doi.org/10.1007/978-3-319-21903-5>
- Nørgaard M, Ganz M, Svarer C, Frokjaer VG, Greve DN, Strother SC, Knudsen GM. 2019. Optimization of preprocessing strategies in Positron Emission Tomography (PET) neuroimaging: A [<sup>11</sup>C]DASB PET study. *NeuroImage* **199**:466–479. DOI: <https://doi.org/10.1016/j.neuroimage.2019.05.055>, PMID: 31158479
- Paquola C, Vos De Wael R, Wagstyl K, Bethlehem RAI, Hong S- J, Seidlitz J, Bullmore ET, Evans AC, Misisic B, Margulies DS, Smallwood J, Bernhardt BC. 2019. Microstructural and functional gradients are increasingly dissociated in transmodal cortices. *PLOS Biology* **17**:e3000284. DOI: <https://doi.org/10.1371/journal.pbio.3000284>, PMID: 31107870
- Pauls DL, Abramovitch A, Rauch SL, Geller DA. 2014. Obsessive- compulsive disorder: an integrative genetic and neurobiological perspective. *Nature Reviews. Neuroscience* **15**:410–424. DOI: <https://doi.org/10.1038/nrn3746>, PMID: 24840803
- Pedregosa F, Varoquaux G, Gramfort A, Michel V, Thirion B, Grisel O. 2023 Scikit- learn: Machine learning in python. Mach Learn PYTHON.

- Pinsonneault JK, Han DD, Burdick KE, Katakai M, Bertolino A, Malhotra AK, Gu HH, Sadee W. 2011. Dopamine transporter gene variant affecting expression in human brain is associated with bipolar disorder. *Neuropsychopharmacology* **36**:1644–1655. DOI: <https://doi.org/10.1038/npp.2011.45>, PMID: 21525861
- Poldrack RA, Mumford JA, Schonberg T, Kalar D, Barman B, Yarkoni T, Sporns O. 2012. Discovering relations between mind, brain, and mental disorders using topic mapping. *PLOS Computational Biology* **8**:e1002707. DOI: <https://doi.org/10.1371/journal.pcbi.1002707>, PMID: 23071428
- Preti MG, Van De Ville D. 2019. Decoupling of brain function from structure reveals regional behavioral specialization in humans. *Nature Communications* **10**:4747. DOI: <https://doi.org/10.1038/s41467-019-12765-7>, PMID: 31628329
- Quah SKL, Mclver L, Roberts AC, Santangelo AM. 2020. Trait anxiety mediated by Amygdala Serotonin transporter in the common marmoset. *The Journal of Neuroscience* **40**:4739–4749. DOI: <https://doi.org/10.1523/JNEUROSCI.2930-19.2020>, PMID: 32393533
- RajMohan V, Mohandas E. 2007. The limbic system. *Indian Journal of Psychiatry* **49**:132. DOI: <https://doi.org/10.4103/0019-5545.33264>
- Rao S, Han X, Shi M, Siu CO, Waye MMY, Liu G, Wing YK. 2019. Associations of the serotonin transporter promoter polymorphism (5-HTTLPR) with bipolar disorder and treatment response: A systematic review and meta-analysis. *Progress in Neuro-Psychopharmacology & Biological Psychiatry* **89**:214–226. DOI: <https://doi.org/10.1016/j.pnpbp.2018.08.035>, PMID: 30217771
- Royer J, Rodríguez- Cruces R, Tavakol S, Larivière S, Herholz P, Li Q, Vos de Wael R, Paquola C, Benkarim O, Park BY, Lowe AJ, Margulies D, Smallwood J, Bernasconi A, Bernasconi N, Frauscher B, Bernhardt BC. 2022. An open MRI dataset for multiscale neuroscience. *Scientific Data* **9**:569. DOI: <https://doi.org/10.1038/s41597-022-01682-y>, PMID: 36109562
- Schaefer A, Kong R, Gordon EM, Laumann TO, Zuo XN, Holmes AJ, Eickhoff SB, Yeo BTT. 2018. Local- global parcellation of the human cerebral cortex from intrinsic functional connectivity MRI. *Cerebral Cortex* **28**:3095–3114. DOI: <https://doi.org/10.1093/cercor/bhx179>, PMID: 28981612
- Schmaal L, Hibar DP, Sämann PG, Hall GB, Baune BT, Jahanshad N, Cheung JW, van Erp TGM, Bos D, Ikram MA, Vernooij MW, Niessen WJ, Tiemeier H, Hofman A, Wittfeld K, Grabe HJ, Janowitz D, Bülow R, Seltonke M, Völzke H, et al. 2017. Cortical abnormalities in adults and adolescents with major depression based on brain scans from 20 cohorts worldwide in the ENIGMA Major Depressive Disorder Working Group. *Molecular Psychiatry* **22**:900–909. DOI: <https://doi.org/10.1038/mp.2016.60>, PMID: 27137745
- Seeman P. 2013. Schizophrenia and dopamine receptors. *European Neuropsychopharmacology* **23**:999–1009. DOI: <https://doi.org/10.1016/j.euroneuro.2013.06.005>
- Shine JM. 2019. Neuromodulatory influences on integration and segregation in the brain. *Trends in Cognitive Sciences* **23**:572–583. DOI: <https://doi.org/10.1016/j.tics.2019.04.002>, PMID: 31076192
- Smallwood J, Brown K, Baird B, Schooler JW. 2012. Cooperation between the default mode network and the frontal- parietal network in the production of an internal train of thought. *Brain Research* **1428**:60–70. DOI: <https://doi.org/10.1016/j.brainres.2011.03.072>, PMID: 21466793
- Smallwood J, Bernhardt BC, Leech R, Bzdok D, Jefferies E, Margulies DS. 2021. The default mode network in cognition: A topographical perspective. *Nature Reviews. Neuroscience* **22**:503–513. DOI: <https://doi.org/10.1038/s41583-021-00474-4>, PMID: 34226715
- Smith H, Elliott J. 2001. Alpha2 receptors and agonists in pain management. *Current Opinion in Anaesthesiology* **14**:513–518. DOI: <https://doi.org/10.1097/00001503-200110000-00009>

- Sokal RR, Michener CD, of KU. 1958. *A statistical method for evaluating systematic relationships* University of Kansas.
- Soomro GM, Altman D, Rajagopal S, Oakley- Browne M. 2008. Selective serotonin re- uptake inhibitors (SSRIs) versus placebo for obsessive compulsive disorder (OCD). *The Cochrane Database of Systematic Reviews*
- 2008:CD001765. DOI: <https://doi.org/10.1002/14651858.CD001765.pub3>, PMID: 18253995
- Sprenghorn RN, Mar RA, Kim ASN. 2009. The common neural basis of autobiographical memory, prospection, navigation, theory of mind, and the default mode: A quantitative meta-analysis. *Journal of Cognitive Neuroscience* **21**:489–510. DOI: <https://doi.org/10.1162/jocn.2008.21029>, PMID: 18510452
- Steinley D. 2004. Properties of the Hubert- Arabie adjusted Rand index. *Psychological Methods* **9**:386–396. DOI: <https://doi.org/10.1037/1082-989X.9.3.386>, PMID: 15355155
- Suárez LE, Markello RD, Betzel RF, Misic B. 2020. Linking structure and function in macroscale brain networks. *Trends in Cognitive Sciences* **24**:302–315. DOI: <https://doi.org/10.1016/j.tics.2020.01.008>, PMID: 32160567
- Sullivan LC, Clarke WP, Berg KA. 2015. Atypical antipsychotics and inverse agonism at 5- HT2 receptors. *Current Pharmaceutical Design* **21**:3732–3738. DOI: <https://doi.org/10.2174/1381612821666150605111236>, PMID: 26044975
- Sun D, Ching CRK, Lin A, Forsyth JK, Kushan L, Vajdi A, Jalbrzikowski M, Hansen L, Villalón- Reina JE, Qu X, Jonas RK, van Amelsvoort T, Bakker G, Kates WR, Antshel KM, Fremont W, Campbell LE, McCabe KL, Daly E, Gudbrandsen M, et al. 2020. Large- scale mapping of cortical alterations in 22q11.2 deletion syndrome: Convergence with idiopathic psychosis and effects of deletion size. *Molecular Psychiatry* **25**:1822–1834. DOI: <https://doi.org/10.1038/s41380-018-0078-5>, PMID: 29895892
- Taylor S. 2013. Molecular genetics of obsessive- compulsive disorder: a comprehensive meta-analysis of genetic association studies. *Molecular Psychiatry* **18**:799–805. DOI: <https://doi.org/10.1038/mp.2012.76>, PMID: 22665263
- Thase ME. 2008. Are SNRIs more effective than SSRIs? A review of the current state of the controversy. *Psychopharmacology Bulletin* **41**:58–85 PMID: 18668017.
- Thomas Yeo BT, Krienen FM, Sepulcre J, Sabuncu MR, Lashkari D, Hollinshead M, Roffman JL, Smoller JW, Zöllei L, Polimeni JR, Fischl B, Liu H, Buckner RL. 2011. The organization of the human cerebral cortex estimated by intrinsic functional connectivity. *Journal of Neurophysiology* **106**:1125–1165. DOI: <https://doi.org/10.1152/jn.00338.2011>
- Thompson PM, Stein JL, Medland SE, Hibar DP, Vasquez AA, Renteria ME, Toro R, Jahanshad N, Schumann G, Franke B, Wright MJ, Martin NG, Agartz I, Alda M, Alhusaini S, Almasy L, Almeida J, Alpert K, Andreassen NC, Andreassen OA, et al. 2014. The ENIGMA Consortium: Large- scale collaborative analyses of neuroimaging and genetic data. *Brain Imaging and Behavior* **8**:153–182. DOI: <https://doi.org/10.1007/s11682-013-9269-5>, PMID: 24399358
- Tian Y, Margulies DS, Breakspear M, Zalesky A. 2020. Topographic organization of the human subcortex unveiled with functional connectivity gradients. *Nature Neuroscience* **23**:1421–1432. DOI: <https://doi.org/10.1038/s41593-020-00711-6>, PMID: 32989295
- Tor D. W. 2011. NeuroSynth: A new platform for large- scale automated synthesis of human functional neuroimaging data. *Frontiers in Neuroinformatics* **5**:e58. DOI: <https://doi.org/10.3389/conf.fninf.2011.08.00058>
- Traag VA, Waltman L, van Eck NJ. 2019. From Louvain to Leiden: Guaranteeing well- connected communities. *Scientific Reports* **9**:5233. DOI: <https://doi.org/10.1038/s41598-019-41695-z>, PMID: 30914743

Valk SL, Xu T, Paquola C, Park B- Y, Bethlehem RAI, Vos de Wael R, Royer J, Masouleh SK, Bayrak Ş, Kochunov P, Yeo BTT, Margulies D, Smallwood J, Eickhoff SB, Bernhardt BC. 2022. Genetic and phylogenetic uncoupling of structure and function in human transmodal cortex. *Nature Communications* **13**:2341. DOI: <https://doi.org/10.1038/s41467-022-29886-1>, PMID: 35534454

van Erp TGM, Walton E, Hibar DP, Schmaal L, Jiang W, Glahn DC, Pearlson GD, Yao N, Fukunaga M,

Hashimoto R, Okada N, Yamamori H, Bustillo JR, Clark VP, Agartz I, Mueller BA, Cahn W, de Zwarte SMC,

Hulshoff Pol HE, Kahn RS, et al. 2018. Cortical brain abnormalities in 4474 individuals with Schizophrenia and 5098 control subjects via the Enhancing Neuro Imaging Genetics through Meta Analysis (ENIGMA) consortium.

*Biological Psychiatry* **84**:644–654. DOI: <https://doi.org/10.1016/j.biopsych.2018.04.023>, PMID: 29960671

van Rooij D, Anagnostou E, Arango C, Auzias G, Behrmann M, Busatto GF, Calderoni S, Daly E, Deruelle C, Di Martino A, Dinstein I, Duran FLS, Durston S, Ecker C, Fair D, Fedor J, Fitzgerald J, Freitag CM, Gallagher L, Gori I, et al. 2018. Cortical and subcortical brain morphometry differences between patients with Autism Spectrum disorder and healthy individuals across the lifespan: Results from the ENIGMA ASD working group. *The American Journal of Psychiatry* **175**:359–369. DOI: <https://doi.org/10.1176/appi.ajp.2017.17010100>, PMID: 29145754

Váša F, Mišić B. 2022. Null models in network neuroscience. *Nature Reviews. Neuroscience* **23**:493–504. DOI: <https://doi.org/10.1038/s41583-022-00601-9>, PMID: 35641793

Vogt C, Vogt O. Allgemeine ergebnisse unserer hirnforschung. Vol. 21. JA Barth; 1919.

von Koskinas CF, Koskinas GN. 1925. *Die Cytoarchitektur Der Hirnrinde Des Erwachsenen Menschen* Springer.

Vos de Wael R, Benkarim O, Paquola C, Larivière S, Royer J, Tavakol S, Xu T, Hong SJ, Langs G, Valk S, Mısıc B, Milham M, Margulies D, Smallwood J, Bernhardt BC. 2020. BrainSpace: A toolbox for the analysis of macroscale gradients in neuroimaging and connectomics datasets. *Communications Biology* **3**:103. DOI: <https://doi.org/10.1038/s42003-020-0794-7>, PMID: 32139786

Whelan CD, Altmann A, Botía JA, Jahanshad N, Hibar DP, Absil J, Alhusaini S, Alvim MKM, Auvinen P, Bartolini E, Berge FPG, Bernardes T, Blackmon K, Braga B, Caligiuri ME, Calvo A, Carr SJ, Chen J, Chen S, Cherubini A, et al. 2018. Structural brain abnormalities in the common epilepsies assessed in a worldwide ENIGMA study.

*Brain* **141**:391–408. DOI: <https://doi.org/10.1093/brain/awx341>, PMID: 29365066

Yarkoni T, Poldrack RA, Nichols TE, Van Essen DC, Wager TD. 2011. Large- scale automated synthesis of human functional neuroimaging data. *Nature Methods* **8**:665–670. DOI: <https://doi.org/10.1038/nmeth.1635>, PMID: 21706013

Yeh CH, Jones DK, Liang X, Descoteaux M, Connelly A. 2021. Mapping structural connectivity using diffusion MRI: Challenges and opportunities. *Journal of Magnetic Resonance Imaging* **53**:1666–1682. DOI: <https://doi.org/10.1002/jmri.27188>, PMID: 32557893

Zilles K, Palomero-Gallagher N. 2001. Cyto-, myelo-, and receptor architectonics of the human parietal cortex. *NeuroImage* **14**:S8–S20. DOI: <https://doi.org/10.1006/nimg.2001.0823>, PMID: 11373127

Zilles K, Palomero-Gallagher N, Grefkes C, Scheperjans F, Boy C, Amunts K, Schleicher A. 2002. Architectonics of the human cerebral cortex and transmitter receptor fingerprints: Reconciling functional neuroanatomy and neurochemistry. *European Neuropsychopharmacology* **12**:587–599. DOI: [https://doi.org/10.1016/s0924-977x\(02\)00108-6](https://doi.org/10.1016/s0924-977x(02)00108-6), PMID: 12468022

Zilles K, Palomero-Gallagher N, Schleicher A. 2004. Transmitter receptors and functional anatomy of the cerebral cortex. *Journal of Anatomy* **205**:417–432. DOI: <https://doi.org/10.1111/j.0021-8782.2004.00357.x>, PMID:

[15610391](https://pubmed.ncbi.nlm.nih.gov/15610391/)

Zilles K, Amunts K. 2009. Receptor mapping: architecture of the human cerebral cortex. *Current Opinion in Neurology* **22**:331–339. DOI: <https://doi.org/10.1097/WCO.0b013e32832d95db>, PMID: [19512925](https://pubmed.ncbi.nlm.nih.gov/19512925/)

Zilles K, Bacha-Trams M, Palomero-Gallagher N, Amunts K, Fiedler AD. 2015. Common molecular basis of the sentence comprehension network revealed by neurotransmitter receptor fingerprints. *Cortex; a Journal Devoted to the Study of the Nervous System and Behavior* **63**:79–89. DOI: <https://doi.org/10.1016/j.cortex.2014.07.007>, PMID: [25243991](https://pubmed.ncbi.nlm.nih.gov/25243991/)

Zilles K, Palomero-Gallagher N. 2017. Multiple transmitter receptors in regions and layers of the human cerebral cortex. *Frontiers in Neuroanatomy* **11**:78. DOI: <https://doi.org/10.3389/fnana.2017.00078>, PMID: [28970785](https://pubmed.ncbi.nlm.nih.gov/28970785/)

### **3 Discussion**

The aim of this work was to investigate the anatomy of the human neurotransmission landscape in the cerebral cortex and subcortical nuclei through the measure of the receptome, assessing its potential functional relevance, and constructing relationships with other brain organizational modes. Overlaps to meta-analytical activation studies and radiological markers of disease were studied. Furthermore, the cortical organization of chemoarchitectural similarity was compared to neuroanatomical findings in functional and structural connectivity, and markers of cytoarchitectural differentiation. Hereby, the novel anatomical mode of chemoarchitectural similarity was both introduced and characterized with respect to other brain mapping modalities.

#### **3.1 Principal gradients in brain organization**

In analyzing the receptome, this study relied heavily on the spatial patterns yielded by principal gradient decomposition (74), a non-linear dimensionality reduction technique employing diffusion embedding (75). Principal gradient decomposition is a meaningful approach to study brain organization. First, the non-linearity of diffusion embedding enables the discovery of relationships between brain areas that conventional linear techniques, such as Principal Component Analysis (PCA), are technically not able to resolve. However, this distinction between linear and non-linear methods was of no relevance for the present study, as the principal axes of the receptome derived when using either PCA or diffusion embedding dimension reduction techniques were close to indistinguishable. Furthermore, modern brain mapping studies often produce high-dimensional outputs, which introduces additional challenges in data storage and handling, computation, and in the analyses itself (76). Principal gradient decomposition can serve as a succinct dimensionality reduction method through generating low-dimensional manifolds that capture important relationships between different brain areas from an originally high-dimensional metric. Correspondingly, the technique has been used to investigate main organizational axes across multiple different modalities of hierarchical brain organization (16,74,77–80).

## **3.2 The organization of cortical chemoarchitecture**

### **3.2.1 Cortical anatomy as defined by chemoarchitectural similarity gradients**

The main axes of cortical chemoarchitectural differentiation described in this work create a novel perspective on the relationship between different regions of the human cortex. The first receptome gradient formed an axis that spans from inferior temporal and occipital lobes towards the pericentral gyri. The second receptome gradient similarly grouped temporal and occipital lobes, as they formed one pole where the gradient was anchored, and transposed these lobes against frontal and prefrontal lobes. The previously introduced grouping between the temporal and occipital lobes was however split up by the third receptome gradient, which firmly placed these two lobes at opposing poles.

Looking deeper into the role of occipital and temporal lobes, visual and limbic functional networks showed significant alignment to the third receptome gradient. Hierarchical agglomerative clustering of functional networks based on their average NTRM density profiles distinguished both visual and limbic networks from other functional networks, complementing autoradiography-derived clustering results (55). This suggests a more unique chemoarchitecture in these areas and may indicate that the chemoarchitectural profiles of visual and limbic networks (standing in for occipital and temporal cortices) are each considerably different from the rest of the cortex but show no great overlap with each other. Rather than being grouped on one gradient pole in the first and second receptome gradient because they are so similar to one another, occipital and temporal cortices are polar because both are highly distinct from the rest of the cortex, However, they are also very different amongst themselves, exemplified by their separation through the third receptome gradient.

### **3.2.2 Functional decoding of chemoarchitectural similarity axes**

The present work also touches upon functional implications of the main cortical chemoarchitectural similarity axes, both through associating receptome gradients with networks of resting-state functional connectivity (as already mentioned for the third gradient in the previous section), as well as the gradient's association with topic-based meta-analytical decoding maps. The first cortical receptome gradient was significantly aligned to the somato-

motor network on its pericentral pole. Correspondingly, it differentiated somato-motor and control functions from facial recognition and abstraction functions. Regarding the second cortical receptome gradient, the present study discovered a significant alignment to the control (or fronto-parietal) network and the default mode network on the frontal anchor, as well as a significant alignment to the visual network at the temporo-occipital anchor. It opposed facial recognition, emotion recognition and abstraction functions to memory and control functions. Next to the already mentioned significant alignments to the visual and limbic functional networks, the third cortical receptome gradient distinguished regions involved in language and auditory processing from areas associated with mental imagery, memory, and attention.

Summarized, chemoarchitectural similarity differentiates along multiple dimensions of cognitive functionality. However, one common theme seems to be the placement of primary and transmodal regions at opposing gradient ends, a finding already observed in autoradiography studies (65). Correspondence across methodologies and scales of resolution strengthens the validity of this finding. Similar results could also be found studying chemoarchitecture in macaques, suggesting that co-occurrence of regional functional and chemoarchitectural specialization is an evolutionary conserved phenomenon (81). Furthermore, systematic distinctions between primary and transmodal regions are also found in cytoarchitectural and FC-based studies (16,77), distinguishing their anatomical differences as an important feature across multiple domains of organization.

### **3.2.3 Disease-related aspects of chemoarchitecture**

This work also associated chemoarchitecture with pathological markers, comparing cortical receptome gradients to disease-associated cortical thinning patterns. Here, the first receptome gradient showed significant correlations to cortical thickness changes observed in obsessive-compulsive disorder, and the second receptome gradient showed significant correlations to alterations of cortical thickness found in patients with bipolar disorder.

Through gradients, transporter and receptor co-distribution profiles can be associated with disease-related alterations in cortical morphology. For the first receptome gradient's

association to obsessive-compulsive disorder, a relationship the gradient creates to the serotonin system is of note, as it is both targeted in its psychopharmacological treatment, as well as implicated in the pathogenesis of obsessive-compulsive disorder. Generally, pharmacological interventions in OCD focus heavily on the serotonin system (82), an important example being Selective Serotonin Reuptake Inhibitors (SSRIs), which target 5-HTT (83,84). Regarding pathogenesis, genetic 5-HT2a and 5-HTT variants constitute risk factors for developing obsessive-compulsive disorder (85), and on the protein level, altered 5-HTT and 5-HT2a functionality in peripheral cells was found in patients with obsessive-compulsive disorder (86).

For the second cortical receptome gradient's association to bipolar disorder, the co-distribution profiles of 5-HTT, DAT and NMDA generated through the gradient are notable, since alterations in these molecules have been found in patients with bipolar disorder. Regarding the glutamatergic NMDA receptor, increased glutamate levels have been detected in patients with bipolar disorder, especially in the frontal cortex (87). Furthermore, several single nucleotide polymorphisms in NMDA receptor subunit genes were significantly enriched in bipolar disorder patient cohorts, and alterations in NMDA receptor binding and mRNA expression of its subunits were reported in multiple cerebral locations in patients with bipolar disorder (88). Similarly, DAT single nucleotide polymorphisms were significantly enriched in patients with bipolar disorder (89), and alterations in dopaminergic neurotransmission could be linked to manic and depressive symptoms in bipolar disorder (90). Finally, changes in 5-HTT receptor binding and genetic 5-HTTLPR polymorphisms have been associated with bipolar disorder genesis (91,92). However, the presented findings that link the aforementioned receptors and transporters to bipolar disorder are sparse. Future studies are needed to investigate and clarify the roles of 5-HTT, NMDA and DAT in bipolar disorder, and to address conflicting results.

As NTRM co-distribution patterns with plausible links to disease phenotypes could be identified through chemoarchitectural similarity gradients, this study proposes that a chemoarchitecturally-driven perspective could provide new avenues to understanding the neurobiological basis of psychiatric and neurological diseases, as has already been shown in recent work studying Parkinson's disease (93). Using chemoarchitectural fingerprints could

account for most psychotropic drugs binding to a variety of receptor and transporter molecules, potentially opening novel paths to a better understanding of psychopharmacological treatments (94–96). Leveraging chemoarchitecture as an anatomical aspect with a clear conceptual connection to clinical medicine could furthermore serve as a bridge into translating more findings from imaging-based neuroanatomy into clinical practice. Especially in psychiatry, a satisfactory translation has not been possible to date. Here, arguably the only relevant finding from imaging-based anatomy that got translated into guideline-based clinical practice thus far is in the domain of repetitive transcranial brain stimulation, where fMRI-based brain mapping identified stimulation targets in the treatment of depression (97,98).

### **3.3 Chemoarchitecture as an anatomical layer**

The current study suggests that chemoarchitectural similarity is organized in a way that partially overlaps with principles of structural, functional, and cytoarchitectural differentiation. This partial overlap is also observed when comparing these other modes amongst each other. For example, the first principal gradients of microstructural profile covariance and functional connectivity correlate at about  $r \sim 0.5$ , and show increasing dissociation towards transmodal cortices as opposed to primary cortices (16). Similarly, overlaps between functional and structural connectivity are a topic of rich and ongoing investigations, since their partial overlap poses fundamental questions regarding signal transmission and processing in the brain (2,72).

It is therefore reassuring to find that chemoarchitecturally-derived cortical topologies show similar partially overlapping characteristics to other measures of hierarchical brain organization. From a theoretical standpoint, it can also be argued that this partial overlap can be expected. Studying hierarchical macro-scale brain organization is only sensible when axiomatically assuming that this hierarchical organization is also instrumental in enabling brain functionality. However, single organizational measures thus far fail to explain brain functionality to a sufficient degree. Finding complete or near-perfect overlaps between different hierarchical organizational measures would thus, as it would introduce only

negligible to no amounts of information, stand against the assumption that hierarchical organization is a key feature in enabling brain functionality. The partial overlaps, where, for example, a sensory-to-association axis of spatial differentiation seems to be given in multiple measures, suggest that there are clear governing principles that underlie general hierarchical organization. Notwithstanding, unique differentiations in every anatomical layer are likely just as important in understanding how the multi-layer, multi-scale composition of the brain holds the key to deciphering its functionality. Therefore, incorporating – among other measures - chemoarchitectural similarity in future studies of structure-function relationships could be crucial in discerning general rules that hierarchical brain architecture adheres to (99). Regarding these general rules, as the subcortical analyses showed that functional communities of subcortical nuclei can be discerned using chemoarchitectural characteristics across multiple modes of analysis, a structure-function relationship between chemoarchitecture and functional specialization known in the cortex (55,62,64,66) could be expanded to subcortical structures. Combined with the general similarity in cortical and subcortical receptomic architecture indicated by the considerable overlaps between cortical and cortico-subcortical receptome gradients, this generalized structure-function relationship could be important to consider in future studies investigating how subcortico-cortical connections modulate functional brain networks (100,101).

### **3.4 Limitations**

There are important limitations to be kept in mind when reading this study. Foremost, it has to be pointed out that not the whole cerebral neurotransmission landscape could be used to assess chemoarchitectural similarity, with relevant molecules, such as the AMPA glutamate receptor, not being part of the primary PET dataset. Future work should expand this study of chemoarchitectural similarity through including more NTRM density maps. Similarly, due to the necessary data not being present in the primary PET dataset, it was not possible to control for effects of current or prior use of medication or previous illnesses. Although NTRM density maps were obtained from healthy participants, density profiles of certain neurotransmitter receptors and transporters can be influenced by both prior psychiatric illnesses as well as prior medication, especially with psychotropic drugs (102,103). As

psychotropic substances also include nicotine, alcohol, and recreational drugs in general, it would also be desirable to control for effects of substance consumption. The findings of the present study have to be interpreted while keeping the limitations pertaining to the primary resource in mind.

Furthermore, the group-averaged datasets employed in this study obfuscate inter-individual differences as an important anatomical and functional aspect that inhomogeneously affects different cortical regions, limiting the transferability of the findings onto the single-subject level especially in transmodal regions (104).

Moreover, analytical decisions have to be kept in mind. In data preprocessing, PET density maps were parcellated according to a functional connectivity-derived atlas, the Schaefer parcellation scheme (105), where vertices are grouped according to pre-defined shared functional connectivity characteristics. While parcellation is a useful dimensionality reduction approach and introduces comparability between different architectural metrics, it is not guaranteed that grouping NTRM density maps based on a functional connectivity atlas is appropriate (106). Future studies might consider using a parcellation derived from cytoarchitectural characteristics (16), as neurotransmitter receptors and transporter have been shown to vary considerably as a function of cytoarchitectural differentiation (54).

Additionally, the conscious decision was made to not differentiate between transporters, ionotropic or metabotropic receptors in creating the receptome, since these molecules reciprocally influence each other's neuromodulatory propensities. As metabotropic signaling can directly influence the neuromodulatory potential of ionotropic receptors (107), and the neuromodulatory potential of presynaptic transporters is directly related to postsynaptic receptor availability, this work makes the argument that, to approximate synaptic signaling complexity in studies of neurochemical anatomy, the incorporation of different receptor types as well as transporters is crucial (1).

Finally, a general limitation of anatomical studies which hypothesize functional implications of the anatomical findings also applies to the present work - the explorative and non-interventional design, where no experiments are performed to validate or falsify a hypothesis. In this work, functional and structural brain anatomical measures were used to contextualize

findings about cortical chemoarchitecture. However, no claims pertaining to causal influences of chemoarchitectural differentiation on functional or structural brain aspects can be made – rather, the contextualization enables a multifaceted and rich characterization of chemoarchitectural anatomy. While hypotheses regarding the relationship between chemoarchitectural features and human functional brain specialization can be extrapolated from the results in this work, establishing a causal rather than a covariance relationship needs a different study design (1).

### **3.5 Conclusion and outlook**

This work outlines the chemoarchitecture of the human cerebral cortex and subcortical structures. It demonstrates meaningful connections to other structural features of brain organization, as well as to functional organization and specialization, and outlines plausible relationships between receptor and transporter co-distribution patterns and morphological alterations found in psychiatric diseases. Furthermore, it finds that relationships between chemoarchitectural anatomy and functional specialization observed in the cortex are also apparent in subcortical nuclei. This study therefore introduces a novel layer of brain structure that shows meaningful connections to other structural as well as functional features in healthy and diseased brains. Incorporating chemoarchitectural similarity in future studies of brain structure-function relationships might thus provide an important advance towards understanding how the brain's seemingly static structure enables functional flexibility. Deciphering this structure-function relationship could prove crucial in a deeper understanding of psychiatric and neurological brain diseases, and open new pathways to their prevention and treatment.

## 4 References

1. Hänisch B, Hansen JY, Bernhardt BC, Eickhoff SB, Dukart J, Misic B, et al. Cerebral chemoarchitecture shares organizational traits with brain structure and function. Forstmann BU, Frank MJ, Medel V, editors. *eLife*. 2023 Jul 13;12:e83843.
2. Suárez LE, Markello RD, Betzel RF, Misic B. Linking Structure and Function in Macroscale Brain Networks. *Trends in Cognitive Sciences*. 2020 Apr 1;24(4):302–15.
3. Brodmann K. *Vergleichende Lokalisationslehre der Grosshirnrinde in ihren Prinzipien dargestellt auf Grund des Zellenbaues*. Barth; 1909.
4. Vogt C, Vogt O. *Allgemeine ergebnisse unserer hirnforschung*. Vol. 21. JA Barth; 1919.
5. Economo C von Koskinas, Georg N. *Die Cytoarchitektonik der Hirnrinde des erwachsenen Menschen*. 1925.
6. Sarkisov SA, Filimonoff IN, Kononowa EP, Preobraschenskaja IS, Kukuev LA. *Atlas of the cytoarchitectonics of the human cerebral cortex*. Moscow: Medgiz. 1955;20.
7. Bailey P. *The isocortex of man*. Urbana. 1951;3.
8. Eickhoff SB, Stephan KE, Mohlberg H, Grefkes C, Fink GR, Amunts K, et al. A new SPM toolbox for combining probabilistic cytoarchitectonic maps and functional imaging data. *NeuroImage*. 2005 May 1;25(4):1325–35.
9. Wree A, Schleicher A, Zilles K. Estimation of volume fractions in nervous tissue with an image analyzer. *Journal of Neuroscience Methods*. 1982 Jul 1;6(1):29–43.
10. Mesulam MM, Hersh LB, Mash DC, Geula C. Differential cholinergic innervation within functional subdivisions of the human cerebral cortex: A choline acetyltransferase study. *Journal of Comparative Neurology*. 1992;318(3):316–28.
11. Hawrylycz MJ, Lein ES, Guillozet-Bongaarts AL, Shen EH, Ng L, Miller JA, et al. An anatomically comprehensive atlas of the adult human brain transcriptome. *Nature*. 2012 Sep;489(7416):391–9.
12. Amunts K, Lepage C, Borgeat L, Mohlberg H, Dickscheid T, Rousseau MÉ, et al. BigBrain: An Ultrahigh-Resolution 3D Human Brain Model. *Science*. 2013 Jun 21;340(6139):1472–5.
13. Glasser MF, Essen DCV. Mapping Human Cortical Areas In Vivo Based on Myelin Content as Revealed by T1- and T2-Weighted MRI. *J Neurosci*. 2011 Aug 10;31(32):11597–616.

14. Ganzetti M, Wenderoth N, Mantini D. Whole brain myelin mapping using T1- and T2-weighted MR imaging data. *Front Hum Neurosci*. 2014 Sep 2;8:671.
15. Royer J, Rodríguez-Cruces R, Tavakol S, Larivière S, Herholz P, Li Q, et al. An Open MRI Dataset for Multiscale Neuroscience [Internet]. *bioRxiv*; 2021 [cited 2022 Apr 14]. p. 2021.08.04.454795. Available from: <https://www.biorxiv.org/content/10.1101/2021.08.04.454795v1>
16. Paquola C, Vos De Wael R, Wagstyl K, Bethlehem RAI, Hong SJ, Seidlitz J, et al. Microstructural and functional gradients are increasingly dissociated in transmodal cortices. *PLOS Biology*. 2019 May;17(5):e3000284.
17. Logothetis NK, Pauls J, Augath M, Trinath T, Oeltermann A. Neurophysiological investigation of the basis of the fMRI signal. *Nature*. 2001 Jul;412(6843):150–7.
18. Logothetis NK. What we can do and what we cannot do with fMRI [Internet]. Vol. 453, *Nature*. Nature Publishing Group; 2008. p. 869–78. Available from: <https://www.nature.com/articles/nature06976>
19. Le Bihan D, Turner R, Zeffiro TA, Cuénod CA, Jezzard P, Bonnerot V. Activation of human primary visual cortex during visual recall: a magnetic resonance imaging study. *Proceedings of the National Academy of Sciences*. 1993 Dec 15;90(24):11802–5.
20. Eden GF, VanMeter JW, Rumsey JM, Maisog JM, Woods RP, Zeffiro TA. Abnormal processing of visual motion in dyslexia revealed by functional brain imaging. *Nature*. 1996 Jul;382(6586):66–9.
21. Dassonville P, Zhu XH, Ugurbil K, Kim SG, Ashe J. Functional activation in motor cortex reflects the direction and the degree of handedness. *Proceedings of the National Academy of Sciences*. 1997 Dec 9;94(25):14015–8.
22. Picard N, Strick PL. Motor Areas of the Medial Wall: A Review of Their Location and Functional Activation. *Cerebral Cortex*. 1996 May 1;6(3):342–53.
23. Corbetta M, Shulman GL. Control of goal-directed and stimulus-driven attention in the brain. *Nat Rev Neurosci*. 2002 Mar;3(3):201–15.
24. Breukelaar IA, Antees C, Grieve SM, Foster SL, Gomes L, Williams LM, et al. Cognitive control network anatomy correlates with neurocognitive behavior: A longitudinal study. *Hum Brain Mapp*. 2016 Sep 13;38(2):631–43.
25. Fletcher PC, Henson RNA. Frontal lobes and human memory: Insights from functional neuroimaging. *Brain*. 2001 May 1;124(5):849–81.
26. Amodio DM, Frith CD. Meeting of minds: the medial frontal cortex and social cognition. *Nat Rev Neurosci*. 2006 Apr;7(4):268–77.

27. Friston KJ. Functional and effective connectivity in neuroimaging: A synthesis. *Human Brain Mapping*. 1994 Jan;2(1–2):56–78.
28. Vossel S, Geng JJ, Fink GR. Dorsal and Ventral Attention Systems. *Neuroscientist*. 2014 Apr;20(2):150–9.
29. Thomas Yeo BT, Krienen FM, Sepulcre J, Sabuncu MR, Lashkari D, Hollinshead M, et al. The organization of the human cerebral cortex estimated by intrinsic functional connectivity. *Journal of Neurophysiology*. 2011 Sep;106(3):1125–65.
30. Buckner RL, Krienen FM, Castellanos A, Diaz JC, Thomas Yeo BT. The organization of the human cerebellum estimated by intrinsic functional connectivity. *Journal of Neurophysiology*. 2011 Nov;106(5):2322–45.
31. Raichle ME. The brain’s default mode network. *Annu Rev Neurosci*. 2015 Jul 8;38:433–47.
32. Lanciego JL, Wouterlood FG. A half century of experimental neuroanatomical tracing. *Journal of Chemical Neuroanatomy*. 2011 Nov 1;42(3):157–83.
33. Bassett DS, Bullmore ET. Small-World Brain Networks Revisited. *Neuroscientist*. 2017 Oct;23(5):499–516.
34. Watts DJ, Strogatz SH. Collective dynamics of ‘small-world’ networks. *Nature*. 1998 Jun;393(6684):440–2.
35. Kim DJ, Min BK. Rich-club in the brain’s macrostructure: Insights from graph theoretical analysis. *Comput Struct Biotechnol J*. 2020 Jun 29;18:1761–73.
36. Heuvel MP van den, Mandl RCW, Stam CJ, Kahn RS, Pol HEH. Aberrant Frontal and Temporal Complex Network Structure in Schizophrenia: A Graph Theoretical Analysis. *J Neurosci*. 2010 Nov 24;30(47):15915–26.
37. Honey CJ, Kötter R, Breakspear M, Sporns O. Network structure of cerebral cortex shapes functional connectivity on multiple time scales. *Proceedings of the National Academy of Sciences*. 2007 Jun 12;104(24):10240–5.
38. Fjell AM, Grydeland H, Krogstad SK, Amlie I, Rohani DA, Ferschmann L, et al. Development and aging of cortical thickness correspond to genetic organization patterns. *Proceedings of the National Academy of Sciences*. 2015 Dec 15;112(50):15462–7.
39. Alexander-Bloch A, Giedd JN, Bullmore E. Imaging structural co-variance between human brain regions. *Nat Rev Neurosci*. 2013 May;14(5):322–36.
40. Thompson PM, Stein JL, Medland SE, Hibar DP, Vasquez AA, Renteria ME, et al. The ENIGMA Consortium: large-scale collaborative analyses of neuroimaging and genetic data. *Brain Imaging and Behavior*. 2014 Jun 1;8(2):153–82.

41. Whelan CD, Altmann A, Botía JA, Jahanshad N, Hibar DP, Absil J, et al. Structural brain abnormalities in the common epilepsies assessed in a worldwide ENIGMA study. *Brain*. 2018 Feb 1;141(2):391–408.
42. Schmaal L, Hibar DP, Sämann PG, Hall GB, Baune BT, Jahanshad N, et al. Cortical abnormalities in adults and adolescents with major depression based on brain scans from 20 cohorts worldwide in the ENIGMA Major Depressive Disorder Working Group. *Mol Psychiatry*. 2017 Jun;22(6):900–9.
43. Erp TGM van, Walton E, Hibar DP, Schmaal L, Jiang W, Glahn DC, et al. Cortical Brain Abnormalities in 4474 Individuals With Schizophrenia and 5098 Control Subjects via the Enhancing Neuro Imaging Genetics Through Meta Analysis (ENIGMA) Consortium. *Biological Psychiatry*. 2018 Nov 1;84(9):644–54.
44. Natu VS, Gomez J, Barnett M, Jeska B, Kirilina E, Jaeger C, et al. Apparent thinning of human visual cortex during childhood is associated with myelination. *Proceedings of the National Academy of Sciences*. 2019 Oct 8;116(41):20750–9.
45. Wagstyl K, Ronan L, Goodyer IM, Fletcher PC. Cortical thickness gradients in structural hierarchies. *NeuroImage*. 2015 May 1;111:241–50.
46. Cahalane DJ, Charvet CJ, Finlay BL. Systematic, balancing gradients in neuron density and number across the primate isocortex. *Front Neuroanat*. 2012 Jul 18;6:28.
47. Eickhoff SB, Bzdok D, Laird AR, Kurth F, Fox PT. Activation Likelihood Estimation meta-analysis revisited. *Neuroimage*. 2012 Feb 1;59(3):2349–61.
48. Yarkoni T, Poldrack RA, Nichols TE, Van Essen DC, Wager TD. Large-scale automated synthesis of human functional neuroimaging data. *Nat Methods*. 2011 Jun 26;8(8):665–70.
49. Poldrack RA, Mumford JA, Schonberg T, Kalar D, Barman B, Yarkoni T. Discovering Relations Between Mind, Brain, and Mental Disorders Using Topic Mapping. *PLOS Computational Biology*. 2012 Oct 11;8(10):e1002707.
50. Poldrack RA, Yarkoni T. From Brain Maps to Cognitive Ontologies: Informatics and the Search for Mental Structure. *Annu Rev Psychol*. 2016;67:587–612.
51. Eickhoff SB, Rottschy C, Kujovic M, Palomero-Gallagher N, Zilles K. Organizational Principles of Human Visual Cortex Revealed by Receptor Mapping. *Cereb Cortex*. 2008 Nov;18(11):2637–45.
52. Nørgaard M, Beliveau V, Ganz M, Svarer C, Pinborg LH, Keller SH, et al. A high-resolution in vivo atlas of the human brain’s benzodiazepine binding site of GABAA receptors. *NeuroImage*. 2021 May 15;232:117878.

53. Eickhoff SB, Rottschy C, Zilles K. Laminar distribution and co-distribution of neurotransmitter receptors in early human visual cortex. *Brain Struct Funct*. 2007 Dec;212(3–4):255–67.
54. Zilles K, Amunts K. Receptor mapping: architecture of the human cerebral cortex. *Current Opinion in Neurology*. 2009 Aug;22(4):331–9.
55. Zilles K, Palomero-Gallagher N. Multiple Transmitter Receptors in Regions and Layers of the Human Cerebral Cortex. *Frontiers in Neuroanatomy* [Internet]. 2017 [cited 2022 Aug 2];11. Available from: <https://www.frontiersin.org/articles/10.3389/fnana.2017.00078>
56. Zilles K, Palomero-Gallagher N. Cyto-, Myelo-, and Receptor Architectonics of the Human Parietal Cortex. *NeuroImage*. 2001 Jul 1;14(1):S8–20.
57. Amunts K, Lenzen M, Friederici AD, Schleicher A, Morosan P, Palomero-Gallagher N, et al. Broca's Region: Novel Organizational Principles and Multiple Receptor Mapping. *PLOS Biology*. 2010 Sep 21;8(9):e1000489.
58. Beliveau V, Ganz M, Feng L, Ozenne B, Højgaard L, Fisher PM, et al. A High-Resolution In Vivo Atlas of the Human Brain's Serotonin System. *J Neurosci*. 2017 Jan 4;37(1):120–8.
59. Dukart J, Holiga S, Rullmann M, Lanzenberger R, Hawkins PCT, Mehta MA, et al. JuSpace: A tool for spatial correlation analyses of magnetic resonance imaging data with nuclear imaging derived neurotransmitter maps. *Human Brain Mapping*. 2021 Feb;42(3):555–66.
60. Zilles K, Palomero-Gallagher N, Schleicher A. Transmitter receptors and functional anatomy of the cerebral cortex. *Journal of Anatomy*. 2004;205(6):417–32.
61. Zilles K, Palomero-Gallagher N, Grefkes C, Scheperjans F, Boy C, Amunts K, et al. Architectonics of the human cerebral cortex and transmitter receptor fingerprints: reconciling functional neuroanatomy and neurochemistry. *European Neuropsychopharmacology*. 2002 Dec 1;12(6):587–99.
62. Morosan P, Schleicher A, Amunts K, Zilles K. Multimodal architectonic mapping of human superior temporal gyrus. *Anat Embryol*. 2005 Dec 1;210(5):401–6.
63. Amunts K, Zilles K. Architectonic Mapping of the Human Brain beyond Brodmann. *Neuron*. 2015 Dec;88(6):1086–107.
64. Dehaene S, Hauser MD, Duhamel JR, Rizzolatti G. From monkey brain to human brain: A Fyssen foundation symposium. MIT press; 2005.
65. Goulas A, Changeux JP, Wagstyl K, Amunts K, Palomero-Gallagher N, Hilgetag CC. The natural axis of transmitter receptor distribution in the human cerebral cortex. *Proceedings of the National Academy of Sciences* [Internet]. 2021 Jan;118(3).

Available from: <https://www.pnas.org/content/118/3/e2020574118>  
<https://www.pnas.org/content/118/3/e2020574118.abstract>

66. Zilles K, Bacha-Trams M, Palomero-Gallagher N, Amunts K, Friederici AD. Common molecular basis of the sentence comprehension network revealed by neurotransmitter receptor fingerprints. *Cortex*. 2015 Feb 1;63:79–89.
67. Hansen JY, Shafiei G, Markello RD, Smart K, Cox SML, Nørgaard M, et al. Mapping neurotransmitter systems to the structural and functional organization of the human neocortex. *Nat Neurosci*. 2022 Nov;25(11):1569–81.
68. Shine JM, van den Brink RL, Hernaus D, Nieuwenhuis S, Poldrack RA. Catecholaminergic manipulation alters dynamic network topology across cognitive states. *Network Neuroscience*. 2018 Sep 1;2(3):381–96.
69. Achard S, Bullmore E. Efficiency and Cost of Economical Brain Functional Networks. *PLOS Computational Biology*. 2007 Feb 2;3(2):e17.
70. Tagliazucchi E, Roseman L, Kaelen M, Orban C, Muthukumaraswamy SD, Murphy K, et al. Increased Global Functional Connectivity Correlates with LSD-Induced Ego Dissolution. *Current Biology*. 2016 Apr 25;26(8):1043–50.
71. Daws RE, Timmermann C, Giribaldi B, Sexton JD, Wall MB, Erritzoe D, et al. Increased global integration in the brain after psilocybin therapy for depression. *Nat Med*. 2022 Apr;28(4):844–51.
72. Uddin LQ. Complex relationships between structural and functional brain connectivity. *Trends in Cognitive Sciences*. 2013 Dec;17(12):600–2.
73. Carhart-Harris RL, Nutt DJ. Serotonin and brain function: A tale of two receptors. *Journal of Psychopharmacology*. 2017 Sep;31(9):1091–120.
74. Vos de Wael R, Benkarim O, Paquola C, Lariviere S, Royer J, Tavakol S, et al. BrainSpace: a toolbox for the analysis of macroscale gradients in neuroimaging and connectomics datasets. *Communications Biology*. 2020 Dec;3(1):1–10.
75. Coifman RR, Lafon S. Diffusion maps. *Applied and Computational Harmonic Analysis*. 2006 Jul 1;21(1):5–30.
76. Mwangi B, Tian TS, Soares JC. A review of feature reduction techniques in neuroimaging. *Neuroinformatics*. 2014 Apr;12(2):229–44.
77. Margulies DS, Ghosh SS, Goulas A, Falkiewicz M, Huntenburg JM, Langs G, et al. Situating the default-mode network along a principal gradient of macroscale cortical organization. *Proceedings of the National Academy of Sciences of the United States of America*. 2016 Nov;113(44):12574–9.

78. Vos de Wael R, Royer J, Tavakol S, Wang Y, Paquola C, Benkarim O, et al. Structural Connectivity Gradients of the Temporal Lobe Serve as Multiscale Axes of Brain Organization and Cortical Evolution. *Cereb Cortex*. 2021 Jun 19;31(11):5151–64.
79. Guell X, Schmahmann JD, Gabrieli JD, Ghosh SS. Functional gradients of the cerebellum. Bostan A, Ivry RB, editors. *eLife*. 2018 Aug 14;7:e36652.
80. Larivière S, Vos de Wael R, Hong SJ, Paquola C, Tavakol S, Lowe AJ, et al. Multiscale Structure–Function Gradients in the Neonatal Connectome. *Cerebral Cortex*. 2020 Jan 10;30(1):47–58.
81. Froudust-Walsh S, Xu T, Niu M, Rapan L, Zhao L, Margulies DS, et al. Gradients of neurotransmitter receptor expression in the macaque cortex. *Nat Neurosci*. 2023 Jul;26(7):1281–94.
82. Pittenger C, Bloch MH. Pharmacological treatment of obsessive-compulsive disorder. *Psychiatr Clin North Am*. 2014 Sep;37(3):375–91.
83. Soomro GM, Altman DG, Rajagopal S, Browne MO. Selective serotonin re-uptake inhibitors (SSRIs) versus placebo for obsessive compulsive disorder (OCD). *Cochrane Database of Systematic Reviews* [Internet]. 2008 [cited 2022 May 2];(1). Available from: <https://www.cochranelibrary.com/cdsr/doi/10.1002/14651858.CD001765.pub3/abstract>
84. Lissemore JI, Sookman D, Gravel P, Berney A, Barsoum A, Diksic M, et al. Brain serotonin synthesis capacity in obsessive-compulsive disorder: effects of cognitive behavioral therapy and sertraline. *Transl Psychiatry*. 2018 Apr 18;8(1):1–10.
85. Taylor S. Molecular genetics of obsessive-compulsive disorder: a comprehensive meta-analysis of genetic association studies. *Mol Psychiatry*. 2013 Jul;18(7):799–805.
86. Delorme R, Betancur C, Callebert J, Chabane N, Laplanche JL, Mouren-Simeoni MC, et al. Platelet Serotonergic Markers as Endophenotypes for Obsessive-Compulsive Disorder. *Neuropsychopharmacol*. 2005 Aug;30(8):1539–47.
87. Hashimoto K, Sawa A, Iyo M. Increased levels of glutamate in brains from patients with mood disorders. *Biol Psychiatry*. 2007 Dec 1;62(11):1310–6.
88. Ghasemi M, Phillips C, Trillo L, De Miguel Z, Das D, Salehi A. The role of NMDA receptors in the pathophysiology and treatment of mood disorders. *Neuroscience & Biobehavioral Reviews*. 2014 Nov 1;47:336–58.
89. Pinsonneault JK, Han DD, Burdick KE, Kataki M, Bertolino A, Malhotra AK, et al. Dopamine Transporter Gene Variant Affecting Expression in Human Brain is Associated with Bipolar Disorder. *Neuropsychopharmacol*. 2011 Jul;36(8):1644–55.

90. Ashok AH, Marques TR, Jauhar S, Nour MM, Goodwin GM, Young AH, et al. The dopamine hypothesis of bipolar affective disorder: the state of the art and implications for treatment. *Mol Psychiatry*. 2017 May;22(5):666–79.
91. Rao S, Han X, Shi M, Siu CO, Waye MMY, Liu G, et al. Associations of the serotonin transporter promoter polymorphism (5-HTTLPR) with bipolar disorder and treatment response: A systematic review and meta-analysis. *Progress in Neuro-Psychopharmacology and Biological Psychiatry*. 2019 Mar 8;89:214–26.
92. Cannon DM, Ichise M, Fromm SJ, Nugent AC, Rollis D, Gandhi SK, et al. Serotonin Transporter Binding in Bipolar Disorder Assessed using [11C]DASB and Positron Emission Tomography. *Biological Psychiatry*. 2006 Aug 1;60(3):207–17.
93. Khan AF, Adewale Q, Lin SJ, Baumeister TR, Zeighami Y, Carbonell F, et al. Patient-specific models link neurotransmitter receptor mechanisms with motor and visuospatial axes of Parkinson’s disease. *Nat Commun*. 2023 Sep 26;14(1):6009.
94. Thase ME. Are SNRIs more effective than SSRIs? A review of the current state of the controversy. *Psychopharmacol Bull*. 2008;41(2):58–85.
95. Sullivan LC, Clarke WP, Berg KA. Atypical Antipsychotics and Inverse Agonism at 5-HT<sub>2</sub> Receptors. *Curr Pharm Des*. 2015;21(26):3732–8.
96. Moraczewski J, Aedma KK. Tricyclic Antidepressants [Internet]. StatPearls [Internet]. StatPearls Publishing; 2022 [cited 2022 Aug 2]. Available from: <https://www.ncbi.nlm.nih.gov/books/NBK557791/>
97. Grimm S, Beck J, Schuepbach D, Hell D, Boesiger P, Birmpohl F, et al. Imbalance between Left and Right Dorsolateral Prefrontal Cortex in Major Depression Is Linked to Negative Emotional Judgment: An fMRI Study in Severe Major Depressive Disorder. *Biological Psychiatry*. 2008 Feb 15;63(4):369–76.
98. Friedman NP, Robbins TW. The role of prefrontal cortex in cognitive control and executive function. *Neuropsychopharmacol*. 2022 Jan;47(1):72–89.
99. García-Cabezas MÁ, Zikopoulos B, Barbas H. The Structural Model: a theory linking connections, plasticity, pathology, development and evolution of the cerebral cortex. *Brain Struct Funct*. 2019 Apr;224(3):985–1008.
100. Bell PT, Shine JM. Subcortical contributions to large-scale network communication. *Neuroscience & Biobehavioral Reviews*. 2016 Dec 1;71:313–22.
101. Janacek K, Evans TM, Kiss M, Shah L, Blumenfeld H, Ullman MT. Subcortical Cognition: The Fruit Below the Rind. *Annual Review of Neuroscience*. 2022;45(1):null.
102. Silvestri S, Seeman MV, Negrete JC, Houle S, Shammi CM, Remington GJ, et al. Increased dopamine D<sub>2</sub> receptor binding after long-term treatment with antipsychotics

- in humans: a clinical PET study. *Psychopharmacology (Berl)*. 2000 Oct;152(2):174–80.
103. Cervenka S, Hedman E, Ikoma Y, Djurfeldt DR, Rück C, Halldin C, et al. Changes in dopamine D2-receptor binding are associated to symptom reduction after psychotherapy in social anxiety disorder. *Transl Psychiatry*. 2012 May;2(5):e120–e120.
  104. Mueller S, Wang D, Fox MD, Yeo BTT, Sepulcre J, Sabuncu MR, et al. Individual variability in functional connectivity architecture of the human brain. *Neuron*. 2013 Feb 6;77(3):586–95.
  105. Schaefer A, Kong R, Gordon EM, Laumann TO, Zuo XN, Holmes AJ, et al. Local-Global Parcellation of the Human Cerebral Cortex from Intrinsic Functional Connectivity MRI. *Cereb Cortex*. 2018 Sep 1;28(9):3095–114.
  106. Eickhoff SB, Yeo BTT, Genon S. Imaging-based parcellations of the human brain. *Nat Rev Neurosci*. 2018 Nov;19(11):672–86.
  107. Neve KA, Seamans JK, Trantham-Davidson H. Dopamine Receptor Signaling. *Journal of Receptors and Signal Transduction*. 2004 Jan 1;24(3):165–205.

## **Danksagung**

Mein besonderer Dank gilt Frau Dr. Sofie L. Valk, welche mich als herausragende direkte Betreuerin bei diesem Projekt unterstützt hat. Darüber hinaus danke ich Herrn Prof. Juergen Dukart für seine Unterstützung als Doktorvater, sowie Herrn Prof. Simon B. Eickhoff, der als Institutsleiter den strukturellen und finanziellen Rahmen zur Durchführung dieser Arbeit zur Verfügung stellte. Neben den bereits genannten Aspekten möchte ich euch gesondert für die exzellente wissenschaftliche Ausbildung, welche ich im Umfeld des Forschungszentrums Jülich durch euch erfahren durfte, und euer großes Engagement herzlich danken.

Mein weiterer Dank gilt den Kollaborationspartnern der McGill University, Frau Justine Y. Hansen, Herrn Prof. Boris C. Bernhardt und Herrn Prof. Bratislav Mistic, für die produktive transatlantische wissenschaftliche Zusammenarbeit.

Darüber hinaus möchte ich den Mitarbeitern des cognitive neurogenetics lab und des INM-7 des Forschungszentrums Jülich für die Unterstützung bei diesem Projekt danken, sowie der Max-Planck-Gesellschaft für die Übernahme der Veröffentlichungskosten des Papers.

Diese Arbeit wäre ohne offen zugängliche Datensätze nicht durchführbar gewesen. Ich möchte allen an der Erstellung, Veröffentlichung und Zugänglichmachung offen zugänglicher Datensätze beteiligten Menschen danken. Hier gilt ein gesonderter Dank den Menschen, die sich als Studienprobanden zur Verfügung stellen.